International Journal of Bifurcation and Chaos, Vol. 29, No. 9 (2019) 1930024 (29 pages)

DOI: 10.1142/S0218127419300246

Lateral Dynamics of Walking-Like Mechanical Systems and Their Chaotic Behavior*

Sergej Čelikovský† and Volodymyr Lynnyk‡
The Czech Academy of Sciences,
Institute of Information Theory and Automation,
Pod vodárenskou věží 4, Prague 8,
182 08, Czech Republic
†*celikovs@utia.cas.cz*
‡*volodymyr.lynnyk@utia.cas.cz*

Received December 11, 2018

A detailed mathematical analysis of the two-dimensional hybrid model for the lateral dynamics of walking-like mechanical systems (the so-called hybrid inverted pendulum) is presented in this article. The chaotic behavior, when being externally harmonically perturbed, is demonstrated. Two rather exceptional features are analyzed. Firstly, the unperturbed undamped hybrid inverted pendulum behaves inside a certain stability region periodically and its respective frequencies range from zero (close to the boundary of that stability region) to infinity (close to its double support equilibrium). Secondly, the constant lateral forcing less than a certain threshold does not affect the periodic behavior of the hybrid inverted pendulum and preserves its equilibrium at the origin. The latter is due to the hybrid nature of the equilibrium at the origin, which exists only in the Filippov sense. It is actually a trivial example of the so-called pseudo-equilibrium [Kuznetsov *et al.*, 2003]. Nevertheless, such an observation holds only for constant external forcing and even arbitrary small time-varying external forcing may destabilize the origin. As a matter of fact, one can observe many, possibly even infinitely many, distinct chaotic attractors for a single system when the forcing amplitude does not exceed the mentioned threshold. Moreover, some general properties of the hybrid inverted pendulum are characterized through its topological equivalence to the classical pendulum. Extensive numerical experiments demonstrate the chaotic behavior of the harmonically perturbed hybrid inverted pendulum.

Keywords: Hybrid system; walking robot; lateral dynamics; chaos.

1. Introduction

The purpose of this paper is to provide the detailed mathematical analysis of the so-called hybrid inverted pendulum including its chaotic behavior when subjected to the external periodic harmonic forcing.

Hybrid inverted pendulum shown in Fig. 2 is a simple one-degree-of-freedom mechanical system introduced in [Čelikovský & Lynnyk, 2018a] to study the lateral dynamics of the three-dimensional underactuated walking-like mechanical system when just two-dimensional walking strategies are applied. Typical two-dimensional walking-like system, or walking robot, can be seen in Fig. 1. The dynamics of the walking robot is studied and controlled in the forward direction only while laterally it is supported by the special frame. Its forward dynamics is still an interesting and challenging topic of the investigation even when omitting the lateral dynamics and their mutual coupling. There are

*Supported by the Czech Science Foundation through the research grant no. 17-04682S.

Fig. 1. The experimental robot in ÚTIA (Institute of Information Theory and Automation) laboratory.

two crucial features to be addressed when designing and analyzing the walking robot: its mathematical model is both under-actuated and hybrid.

The under-actuation is related to the fact that the robotic device shown in Fig. 1 does not include the actuated ankles and therefore the pivot angle between the stance leg and the ground is not actuated. In such a way, any model of the swing phase of the walking should have less independent actuators than degrees of freedom. Recall in this context that the mechanical systems having less actuators than degrees of freedom are called *under-actuated mechanical systems*. On the contrary, fully actuated robots use large flat feet and the strong ankles actuation with the necessity to preserve the full contact of the feet with the ground via the so-called zero moment point computation. In such a way, the under-actuated walking more adequately represents the intrinsic essence of the human gait where the ankles cannot provide a large torque and stability is maintained thanks to a dynamic essence of the movement. See famous *IEEE Control Systems Magazine* paper [Chevallereau *et al.*, 2003] for more arguments and some historical remarks.

As already noted, only the sagittal plane dynamics is modeled during the planar walking assuming that the lateral stability is ensured by some *ad hoc* supporting frame, rod, moving platform, etc. For some representative yet not complete picture see e.g. the monographs [Westervelt *et al.*, 2007; Chevallereau *et al.*, 2009], or the general introductory part of a more recent paper [Grizzle *et al.*, 2014] and the references within. Samples of other approaches to planar underactuated walking are [Shiriaev *et al.*, 2014, 2006, 2005; Song & Zefran, 2006a, 2006b; Majumdar *et al.*, 2013; Pchelkin *et al.*, 2015; Spong & Bullo, 2005; La Herra *et al.*, 2013; Dolinský & Čelikovský, 2012, 2018; Čelikovský & Anderle, 2016, 2017].

Yet, fully autonomous walking robots cannot use any supporting frames and require the full three-dimensional walking models being much more complex than the planar ones. Indeed, they require a proper definition of Euler angles and tensors of inertia for each link. See [Song & Zefran, 2006b] for a brief introduction or [Grizzle *et al.*, 2014] for a more comprehensive exposition.

An alternative and somehow simpler treatment was presented in [Kuo, 1999] studying the possibilities to stabilize properly the lateral dynamics independently of the forward one. Still, some active tools were required in [Kuo, 1999] while in [Čelikovský & Lynnyk, 2018a] the authors considered just the natural stability of lateral oscillations, moreover, it is shown to be preserved even under additional limited external harmonic forcing that emulates influence of the coupling with the forward dynamics. The model to study these effects was called the *hybrid inverted pendulum* (*HIP*) in [Čelikovský & Lynnyk, 2018a]. This paper also briefly noted the possible chaotic behavior in the harmonically perturbed HIP and some preliminary study of these chaotic phenomena was presented in [Čelikovský & Lynnyk, 2018b]. In such a way, the HIP belongs to the class of hybrid, or discontinuous Filippov-like systems where these aspects have been broadly studied as well. In particular, period doubling in a simple walking model was demonstrated in [Garcia *et al.*, 1998], while [Shi *et al.*, 2013] and [Dua & Marathe, 2015] presented the Melnikov method for the detection of chaos in nonsmooth systems. In [Kunze, 2000] the Lyapunov exponents for nonsmooth dynamical systems with an application to a pendulum with dry friction are calculated and Li *et al.* [2016a, 2016b] obtained Melnikov function to study the persistence of heteroclinic cycles for a planar hybrid piecewise-smooth system. Bifurcations in discontinuous mechanical systems are studied in detail in [Leine *et al.*, 2000; Leine & Nijmeijer, 2004], while the one-parameter bifurcations in planar Filippov systems were studied in [Kuznetsov *et al.*, 2003]. Several regular and chaotic modes of the sinusoidally driven rigid planar pendulum were discussed and illustrated by the computer simulations in [Butikov, 2008].

As a matter of fact, the above topics go back to the well-known treatment of the passive walkers walking down the moderate slope, where the impact effects are crucial, broadly studied since the seminal paper [McGeer, 1990], cf. more recent results in [Freidovich *et al.*, 2009] and references within. It is well-known that the passive biped walker walking down the slope may exhibit chaotic behavior when the slope is too steep.

The HIP is a particular case of planar Filippov systems classified in [Kuznetsov *et al.*, 2003]. Yet, it deserves further detailed analysis thanks to its practical importance explained above. The main contribution of the present paper is therefore the detailed mathematical analysis of the basic properties of the HIP, including their full mathematical proofs. Further, topological equivalence of the HIP to the linear oscillator is proved to provide some clues to understand the essence of the possible chaotic behavior in the harmonically perturbed HIP. Nevertheless, the proved topological equivalence is of special interest as it relates the planar Filippov system having the discontinuous right-hand side to the planar system having the smooth right-hand side. Finally, the detailed numerical experiments are performed to demonstrate how and why chaos appears, in particular, the relation between the forcing amplitude and frequency and the size of the chaotic oscillations.

More specifically, two types of situations will be observed. First, for the amplitudes not exceeding certain threshold, chaos requires sufficiently large initial condition, i.e. it does not attract the trajectories starting at the origin or very close to it. Moreover, there are many attractors, each of them is reached only from a specific and limited basin of attraction. In such a way, **multiple hidden attractors** in the sense of Leonov–Kuznetsov [Leonov *et al.*, 2011; Leonov & Kuznetsov, 2013; Chen *et al.*, 2017] are observed in this case. Secondly, for the amplitudes larger than the threshold, the HIP exhibits the chaotic behavior even for a very small (practically zero) initial condition and the size of the attractor depends on the forcing frequency, i.e. a smaller forcing frequency generates a larger attractor and *vice versa*.

The rest of the paper is organized as follows. The next section introduces the HIP, its state space model and provides the mathematical results on existence and uniqueness if its solutions, stability, etc., including the detailed mathematical proofs. Section 3 provides further analysis through topological equivalence that may help to understand the chaos emergence in the harmonically perturbed undamped HIP. Section 4 presents the experimental numerical simulations-based investigation and some conjectures based on them. The final section contains concluding ideas.

Notation. Euclidean norm in $\mathbb{R}^n$ is denoted as $\|\cdot\|$, $\mathcal{B}_{c,r} := \{x \in \mathbb{R}^n \,|\, \|x - c\| < r\}$, $\operatorname{sign}(a) = a/|a|$, $a \neq 0$, $\operatorname{sign}(0) = 0$, and $g = 9.81$ is the gravity constant. COM stands for the center of mass, DOF for the degree of freedom, MI for the moment of inertia. Moreover, $\operatorname{Sign}(x)$ is the set-valued map with $\operatorname{Sign}(a) = \{\operatorname{sign}(a)\}$, $a \neq 0$ and $\operatorname{Sign}(0) = [-1, 1]$. For a mapping $f : \mathbb{R}^n \mapsto \mathbb{R}^n$ and a set $\Omega \subset \mathbb{R}^n$ denote $f(\Omega) := \{z \in \mathbb{R}^n \,|\, \exists\, x \in \mathbb{R}^n : f(x) = z\}$. Furthermore, for a set $\Omega \subset \mathbb{R}^n$ denote its closure in Euler norm topology as $\overline{\Omega}$ and its convex hull as $\operatorname{co}(\Omega)$. For brevity, $\overline{\operatorname{co}}\Omega$ stands for the convex closure, i.e. $\overline{\operatorname{co}}\Omega := \overline{\operatorname{co}(\Omega)}$. Finally, denote $\dot{x} := \mathrm{d}x/\mathrm{d}t$.

2. Hybrid Inverted Pendulum Model and Its Properties

The hybrid inverted pendulum (HIP) is depicted in Fig. 2. Its mechanical configuration is more complex than the one presented in [Čelikovský & Lynnyk, 2018b] and it also more adequately mimics the real laboratory model shown in Fig. 1. It is composed from the left link, the right link, the upper link and the torso. All these elements are attached to each other rigidly and perpendicularly. They are assumed to be narrow homogeneous rods with some additional masses placed on them. In such a

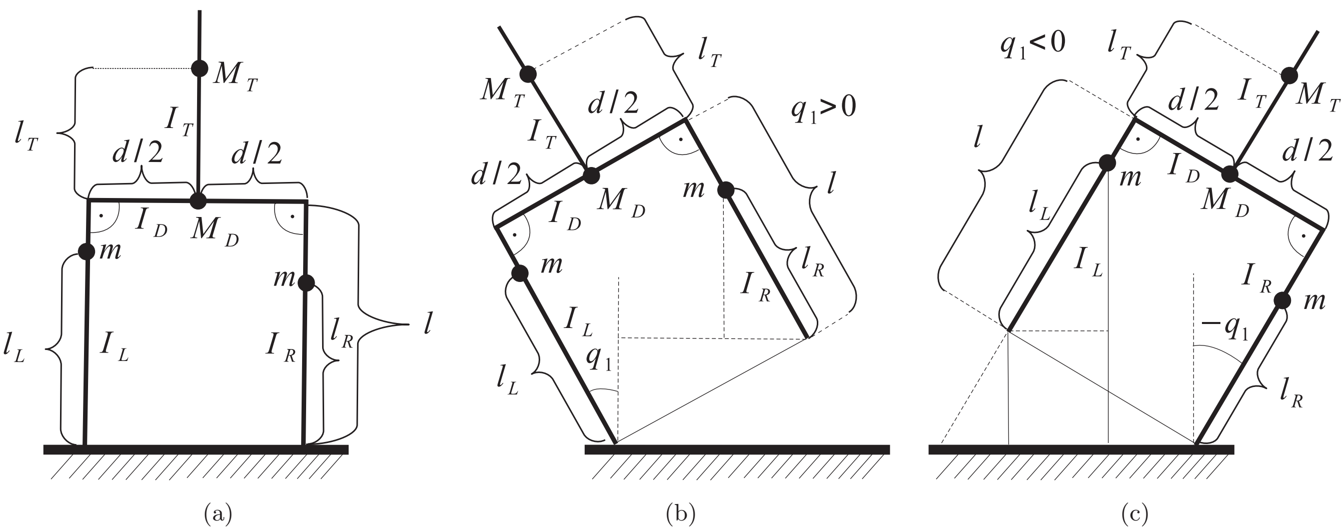

Fig. 2. Hybrid inverted pendulum. (a) $q_1 = 0$, (b) $q_1 > 0$ and (c) $q_1 < 0$.

way, they are modeled using their overall masses placed at the appropriate COMs and their MIs with respect to the rotation axes passing through those COMs perpendicularly to the plane containing the HIP. The left and right links have the same mass m, but possibly different MIs denoted I_L, I_R and possibly different COMs placement given by the distances l_L, l_R, respectively. The latter feature is due to the fact that the HIP actually emulates the frontal projection of the robot shown in Fig. 1, having straightened legs at knees, but both these legs need not belong to the frontal plane, or even to a single plane. The upper link has the length d, the moment of inertia I_D and the mass M_D, the torso has the moment of inertia I_T, the total mass M_T and the center of mass placement at the distance l_T from the middle of the upper link. Note, that the torso of the real laboratory model in Fig. 1 may have a position not belonging to the frontal plane.

The HIP has a single DOF being the angular displacement q_1 shown in Figs. 2(b) and 2(c), while $\dot{q}_1$ stands for the corresponding angular velocity. To obtain the HIP dynamical model, consider the Lagrangian

$$\mathcal{L} = \mathcal{K} - \mathcal{V}, \quad \mathcal{V} = \theta_1 \cos q_1 + \theta_2 |\sin q_1|, \;\; \mathcal{K} = \frac{\theta \dot{q}_1^2}{2}, \tag{1}$$

$$\begin{aligned} \theta_1 &= g(m(l_L + l_R) + M_D l + M_T(l + l_T)), \\ \theta_2 &= gd\left(m + \frac{M_D + M_T}{2}\right), \end{aligned} \tag{2}$$

$$\begin{aligned} \theta &= m(l_L^2 + l_R^2 + d^2) + I_L + I_R + I_D + I_T \\ &\quad + M_D\left(l^2 + \frac{d^2}{4}\right) + M_T\left((l + l_T)^2 + \frac{d^2}{4}\right), \end{aligned} \tag{3}$$

where $\mathcal{V}$ is the potential energy with respect to the ground level and $\mathcal{K}$ is the kinetic energy with respect to the inertial system stuck to the ground. Note, that the Lagrangian (1) is not smooth for $q_1 = 0$, i.e. the hybrid dynamical model is needed, which justifies the term "HIP". Using the well-known Euler–Lagrange formalism

$$\frac{\mathrm{d}}{\mathrm{d}t}\frac{\partial \mathcal{L}}{\partial \dot{q}_1} - \frac{\partial \mathcal{L}}{\partial q_1} = F(t),$$

where $F(t)$ stands for a possible additional external generalized force, one gets

$$\ddot{q}_1 = \theta^{-1}(\theta_1 \sin q_1 - \theta_2 \mathrm{sign}(q_1) \cos q_1 + F(t)), \quad q_1 \neq 0. \tag{4}$$

Since the generalized coordinate is the angle (i.e. dimensionless physical quantity), the generalized force should be the torque. Indeed, the product of any generalized coordinate and the corresponding generalized force should always have physical dimension Nm. In such a way, $F(t)$ is a certain external torque applied to the HIP, this torque is always acting with respect to the support pivot point of the HIP.

Equation (4) is not valid for $q_1 = 0$ and therefore some switching conditions are needed for $q_1 = 0$. They can be obtained by analyzing the so-called impact, i.e. the effect of one of the vertical links hitting the ground for $q_1 = 0$. The standard assumptions made for the impact are: (i) no leg slipping and rebound; (ii) the impact is instantaneous; (iii) both the total momentum and the total energy are preserved. As the HIP possesses a single degree of freedom only, the switching conditions are simple: both q_1 and $\dot{q}_1$ should stay continuous when switching between $q_1 > 0$ and $q_1 < 0$ in (4). In other words, (4) actually constitutes the system of the second-order differential equations with the discontinuous right-hand side. Nevertheless, the following equivalent treatment in the hybrid setting is possible:

$$q > 0: \ \ddot{q} = \theta^{-1}\theta_1 \sin(q) - \theta^{-1}\theta_2 \cos(q) + \theta^{-1}F(t); \tag{5}$$

$$q = 0: \ q^+ = -q^-, \quad \dot{q}^+ = -\dot{q}^-. \tag{6}$$

In this hybrid setting, q is always positive during the continuous-time part (5), namely, $q := q_1$ in Fig. 2(b) and $q := -q_1$ in Fig. 2(c). Discrete-time part (6) then adequately relabels q and reverses for $q = 0$ the velocity, keeping thereby the set $q \geq 0$ invariant with respect to (5) and (6). In the sequel, the discontinuous right-hand side description (4) will be used, nevertheless, the hybrid setting (5) and (6) justifies yet another time the previously introduced terminology "HIP". Summarizing, one has the following definition.

Definition 2.1. System (4) is called **hybrid inverted pendulum (HIP)**. Its trajectory is defined as everywhere continuously differentiable and almost everywhere second-order continuously differentiable function $q_1(t)$ satisfying (4) for $q_1 \neq 0$. If $F(t) \equiv 0$ ($F(t) \not\equiv 0$), (4) is called as the unforced (forced) HIP.

Further, denote $x_1 = q_1$, $x_2 = \dot{q}_1$ and assume that the external forces have the form $F(t) = -k\dot{q}_1 + w(t)$, $k \geq 0$, where the first term is the friction-like damping while the second one is the bounded external forcing. Denote $\omega(t) = w(t)\theta^{-1}$, $k_1 = k\theta^{-1}$, then (4) gives for $x_1 \neq 0$ the following system of the first-order ordinary differential equations [recall (2), (3) for the definition of constants $\theta, \theta_1, \theta_2$]:

$$\begin{aligned} \dot{x}_1 &= x_2, \\ \dot{x}_2 &= \frac{\theta_1 \sin x_1 - \theta_2 \mathrm{sign}(x_1) \cos x_1}{\theta} \\ &\quad - k_1 x_2 + \omega(t), \quad k_1 \geq 0, \end{aligned} \tag{7}$$

having its right-hand side discontinuous at $x_1 = 0$. System (7) will be called in the sequel **hybrid inverted pendulum in the state space form (HIPSF)**. The HIPSF is called damped (undamped) for $k_1 > 0$ ($k_1 = 0$) and perturbed (unperturbed) for $\omega(t) \not\equiv 0$ ($\omega(t) \equiv 0$). There are two standard saddle point equilibria of the HIPSF for $\omega(t) \equiv 0$:

$$\begin{aligned} x_1^{E_1} &= \arctan(\theta_2\theta_1^{-1}), \quad x_2^{E_1} = 0, \\ x_1^{E_2} &= \arctan(-\theta_2\theta_1^{-1}) = -x_1^{E_1}, \quad x_2^{E_2} = 0. \end{aligned} \tag{8}$$

The following relations for $x_1^{E_1}, x_1^{E_2}$ to be used later are the straightforward consequence of (8):

$$\begin{aligned} \sin^2 x_1^{E_{1,2}} &= \frac{\theta_2^2}{\theta_1^2 + \theta_2^2}, \\ \cos^2 x_1^{E_{1,2}} &= \frac{\theta_1^2}{\theta_1^2 + \theta_2^2}. \end{aligned} \tag{9}$$

Intuitively, it is clear that the HIPSF should have yet another equilibrium at the origin $(0, 0)^\top$ corresponding to its double support and the zero velocity. Despite its clear mechanical meaning, this equilibrium is tractable only as the trivial solution of the differential equation with discontinuous right-hand side (7) in the Filippov sense. In the sequel it will be called as the *equilibrium in the Filippov sense.* To be more specific, let us first recall the following definition.

Definition 2.2. Consider the following ordinary differential equation

$$\dot{x} = f(x), \quad x \in \mathbb{R}^n,$$

where $f(x)$ is bounded on any bounded subset of $\mathbb{R}^n$ and it is smooth except for some submanifold of $\mathbb{R}^n$ where it may be discontinuous. Then its solution in the Filippov sense [Filippov, 1988] on some bounded time interval $[0, T]$, $T > 0$, is an absolutely continuous time function $x(t)$ defined on $[0, T]$, $T > 0$, such that the following differential inclusion

$$\dot{x} \in F(x), \quad F(x) := \bigcap_{\varepsilon > 0} \overline{\mathrm{co}} f(\mathcal{B}_{x,\varepsilon})$$

holds almost everywhere on $[0, T]$. The solution in the Filippov sense $x(t)$ on $[0, T]$, $T > 0$, is called the maximal solution in the Filippov sense if there does not exist a solution $\overline{x}(t)$ on $[0, T']$, $T' > T$, such that $x(t) = \overline{x}(t)$, $\forall\, t \in [0, T]$. If, in addition, $x(0) = x_0$,

$x_0 \in \mathbb{R}^n$, then $x(t)$ is called the solution in the Filippov sense with the initial conditions $x(0) = x_0$. The solution is called globally defined (or simply global), if there is no maximal solution on some bounded interval $[0, T]$, $T > 0$. If there is a trivial solution in the Filippov sense $x(t) = x_0 \in \mathbb{R}^n$, $\forall\, t \geq 0$, then this solution will either be called the equilibrium in the Filippov sense, or the pseudo-equilibrium as in [Kuznetsov *et al.*, 2003]. Analogously, one can define the solutions in the Filippov sense with the initial conditions $x(0) = x_0$ on any time interval $[T_1, T_2]$, $T_1 < 0$, $T_2 > 0$, or on $(-\infty, \infty)$. The latter may be alternatively referred to as the Filippov solution existing for $\forall\, t \in \mathbb{R}$.

Example 2.1. The solution of the scalar ordinary differential equation with the discontinuous right-hand side $\dot{x} = \mathrm{sign}(x)$, $x \neq 0$, in the Filippov sense is the solution of the differential inclusion $\dot{x} \in \mathrm{Sign}(x)$. Note, that the origin is the equilibrium in the Filippov sense only. Moreover, there is no uniqueness of the solution with the initial condition $x(0) = 0$ on $[0, T]$, $\forall\, T > 0$, namely, besides the trivial solution there are two more solutions $x(t) \equiv t$ and $x(t) \equiv -t$. Nevertheless, the similar system $\dot{x} = -\mathrm{sign}(x)$, $x \neq 0$, has the unique solution in the Filippov sense with the initial condition $x(0) = 0$ on $[0, T]$, $\forall\, T > 0$. Let us briefly sketch the proof of this property. Consider the function $x^2/2$ and let $x(t)$ be a solution, then $(\mathrm{d}/\mathrm{d}t)(x^2(t)/2) = -|x(t)| \leq 0$. In such a way, $x^2(t)$ is a nonincreasing function of time in every neighborhood of the origin (except the origin itself) and therefore every absolutely continuous solution starting at the origin cannot leave it. The analogous idea as in the previous sketch will be used later on when analyzing the uniqueness of solutions for the HIPSF.

One can see straightforwardly that

$$\bigcap_{\varepsilon > 0} \overline{\mathrm{co}} f(\mathcal{B}_{x,\varepsilon}) = \{f(x)\}$$

for every point $x \in \mathbb{R}^n$ where $f(x)$ is continuous. As a consequence, the dynamics (7) is for $x_1 \neq 0$ represented in the Filippov sense by the trivial single point set differential inclusion, i.e. by the differential equation

$$\begin{aligned} \dot{x}_1 &= x_2, \\ \dot{x}_2 &= \frac{\theta_1 \sin x_1 - \theta_2 \mathrm{sign}(x_1) \cos x_1}{\theta} \\ &\quad - k_1 x_2 + \omega(t), \quad k_1 \geq 0, \;\; x_1 \neq 0, \end{aligned} \tag{10}$$

while for $x_1 = 0$, it takes the form

$$\begin{aligned} \dot{x}_1 &= x_2, \\ \dot{x}_2 &\in \left[-\frac{\theta_2}{\theta} - k_1 x_2 + \omega(t), \frac{\theta_2}{\theta} - k_1 x_2 + \omega(t) \right], \\ &\qquad k_1 \geq 0, \;\; x_1 = 0. \end{aligned} \tag{11}$$

Proposition 1. *Let $\omega(t) \equiv 0$. Then the mapping $x(t) \equiv (0, 0)^\top, t \in [0, \infty)$, is the global solution of (7) in the Filippov sense with the initial conditions $(0, 0)^\top$. Moreover, any solution of (7) in the Filippov sense $\bar{x}(t)$, $t \in [0, T]$, $T > 0$, $\bar{x}(0) = (0, 0)^\top$, satisfies $\bar{x}(t) \equiv (0, 0)^\top$, $\forall\, t \in [0, T]$.*

Proof. First, note that the mapping $x(t) \equiv (0, 0)^\top$ is obviously the global solution of (7) in the Filippov sense for the initial conditions $(0, 0)^\top$. Indeed, the differential inclusion (11) for $x_1 = x_2 = 0$ and $\omega(t) \equiv 0$ takes the following form

$$\dot{x}_1 = 0, \quad \dot{x}_2 \in \left[-\frac{\theta_2}{\theta}, \frac{\theta_2}{\theta} \right],$$

and therefore $\dot{x}_1(t) = 0, \dot{x}_2(t) = 0$ satisfies that inclusion for all $t \in \mathbb{R}$ since $0 \in [-\theta_2/\theta, \theta_2/\theta]$.

It remains to prove that if $\bar{x}(t)$, $t \in [0, T]$, $T > 0$, with $\bar{x}(0) = (0, 0)^\top$ is the solution of the differential inclusion (10), (11), then $\bar{x}(t) = (0, 0)^\top, \forall\, t \in [0, T]$. To prove this claim, assume the opposite, namely, assume that there exist $t' > 0$, $\varepsilon \in (0, \arctan(\theta_2 \theta_1^{-1}))$ and absolutely continuous mapping $\bar{x}(t)$, $t \in [0, T]$, $T > 0$, satisfying almost everywhere (10), (11), such that $\bar{x}(0) = 0$ and $\varepsilon > \|\bar{x}(t')\| > \varepsilon/2$. Further, consider the following everywhere continuous and differentiable for all $x_1 \neq 0$ function

$$\begin{aligned} V(x_1, x_2) &:= \theta_1(\cos x_1 - 1) + \theta_2 |\sin x_1| + \frac{\theta x_2^2}{2}, \\ &V(x) > 0 \quad \text{for } x \neq 0, \\ &|x_1| < \arctan(\theta_2 \theta_1^{-1}), \quad V(0, 0) = 0. \end{aligned}$$

Indeed, one has straightforwardly that

$$\begin{aligned} &x_1 \frac{\partial V}{\partial x_1} > 0 \quad \forall\, x_1 \neq 0, \;\; |x_1| < \arctan(\theta_2 \theta_1^{-1}), \\ &x_2 \frac{\partial V}{\partial x_2} > 0 \quad \forall\, x_2 \in \mathbb{R} \backslash \{0\}. \end{aligned}$$

Moreover, the function $V(\bar{x}(t)) : \mathbb{R} \mapsto \mathbb{R}$ is absolutely continuous. Indeed, by the definition of the solution, $\overline{x}(t)$ is required to be an absolutely continuous map while $V(x)$ is differentiable $\forall\, x_1 \neq 0$ and by (10) the equality $\overline{x}_1(t) = 0$ may hold at isolated points only due to the *ad absurdum* assumption $\varepsilon > \|\overline{x}(t')\| > \varepsilon/2$, $\varepsilon > 0$. Therefore the time derivative of $V(\overline{x}(t)) : \mathbb{R} \mapsto \mathbb{R}$ exists almost everywhere and straightforward computations show that almost everywhere it holds

$$\frac{\mathrm{d}V(\overline{x}(t))}{\mathrm{d}t} = -k_1 x_2^2 \leq 0.$$

The latter inequality and $V(0,0) = 0$ actually imply that $V(\overline{x}(t')) \leq 0$. Indeed:

$$\begin{aligned} V(\overline{x}(t')) &= V(\overline{x}(t')) - V(0,0) \\ &= V(\overline{x}(t')) - V(\overline{x}(0)) \\ &= \int_0^{t'} \frac{\mathrm{d}V(\overline{x}(s))}{\mathrm{d}s}\mathrm{d}t \leq 0. \end{aligned}$$

Nevertheless, by the *ad absurdum* assumption $\varepsilon > \|\overline{x}(t')\| > \varepsilon/2$, $\varepsilon > 0$, and by the mentioned positive definiteness of the function V, it holds that $V(\overline{x}(t')) > 0$, which is the contradiction. ■

Proposition 2. *Let $\omega(t)$ be a piecewise continuous function such that*

$$\begin{aligned} &\Omega_{\min} \leq \omega(t) \leq \Omega_{\max}, \quad t \in [0,\infty), \\ &\qquad\qquad \Omega_{\min} \in \mathbb{R},\ \ \Omega_{\max} \in \mathbb{R}. \end{aligned} \tag{12}$$

If $[\Omega_{\min}, \Omega_{\max}] \subset [-\theta_2/\theta, \theta_2/\theta]$, then the mapping $x(t) \equiv (0,0)^\top, t \in [0,\infty)$, is the global solution of (7) in the Filippov sense with the initial conditions $(0,0)^\top$. Moreover, if $\omega(t) = \Omega_c \in \mathbb{R}$, $\forall\, t \geq 0$, then any solution of (7) in the Filippov sense $\overline{x}(t)$, $t \in [0,T]$, $T > 0$, $\overline{x}(0) = (0,0)^\top$, satisfies $\overline{x}(t) = (0,0)^\top$, $\forall\, t \in [0,T]$.

Proof. First, note that the mapping $x(t) \equiv (0,0)^\top$ is obviously the solution of (7) in the Filippov sense for the initial conditions $(0,0)^\top$. Indeed, the differential inclusion (11) takes the form for $x_1 = x_2 = 0$ as

$$\dot{x}_1 = 0, \quad \dot{x}_2 \in \left[-\frac{\theta_2}{\theta} + \omega(t), \frac{\theta_2}{\theta} + \omega(t)\right],$$

i.e. $\dot{x}_1(t) = 0$, $\dot{x}_2(t) = 0$ satisfy that inclusion for all $t \in \mathbb{R}$ since by $[\Omega_{\min}, \Omega_{\max}] \subset [-\theta_2/\theta, \theta_2/\theta]$ holds

$$\begin{aligned} 0 &\in \left[-\frac{\theta_2}{\theta} + \Omega_{\max}, \frac{\theta_2}{\theta} + \Omega_{\min}\right] \\ &\subset \left[-\frac{\theta_2}{\theta} + \omega(t), \frac{\theta_2}{\theta} + \omega(t)\right]. \end{aligned}$$

It remains to prove that if $\omega(t) = \Omega_c \in \mathbb{R}$, $\forall\, t \geq 0$, then any solution of the differential inclusion (10), (11), $\overline{x}(t)$, $t \in [0,T]$, $T > 0$, with $\overline{x}(0) = (0,0)^\top$ satisfies $\overline{x}(t) \equiv (0,0)^\top$, $t \in [0,T]$. Assume the opposite, namely, assume that there exist $\varepsilon_0 > 0$ and absolutely continuous mapping $\overline{x}(t)$, $t \in [0,T]$, $T > 0$, satisfying (10), (11) such that $\overline{x}(0) = 0$ and $\|\overline{x}(t')\| > \varepsilon_0$. As a matter of fact, the latter is by the continuity of $\overline{x}(t)$ equivalent to the following property: for all $\varepsilon \in [0, \varepsilon_0)$ there exists $t''(\varepsilon)$ such that $\|\overline{x}(t''(\varepsilon))\| = \varepsilon$.

To show the contradiction, consider the absolutely continuous function

$$\begin{aligned} \overline{V}(x_1, x_2) &:= \theta_1(\cos x_1 - 1) + \theta_2|\sin x_1| \\ &\qquad - \theta\Omega_c x_1 + \frac{\theta x_2^2}{2}, \\ \overline{V}(0,0) &= 0. \end{aligned}$$

Straightforward differentiation and the proposition assumption $\Omega_c \in [\Omega_{\min}, \Omega_{\max}] \subset [-\theta_2/\theta, \theta_2/\theta]$ give

$$\begin{aligned} &\lim_{x_1 \to 0^+} \frac{\partial}{\partial x_1}(\theta_1(\cos x_1 - 1) + \theta_2|\sin x_1| - \theta\Omega_c x_1) \\ &\quad = \theta_2 - \theta\Omega_c > 0, \\ &\lim_{x_1 \to 0^-} \frac{\partial}{\partial x_1}(\theta_1(\cos x_1 - 1) + \theta_2|\sin x_1| - \theta\Omega_c x_1) \\ &\quad = -\theta_2 - \theta\Omega_c < 0. \end{aligned}$$

As a consequence, there exists $\delta > 0$ such that $\overline{V}(x_1, x_2) > 0\ \forall\, x = (x_1, x_2)^\top \neq 0, \|x\| < \delta$. Moreover, straightforward computations show that

$$\frac{\mathrm{d}\overline{V}(\overline{x}(t))}{\mathrm{d}t} = -k_1 x_2^2 \leq 0.$$

The previous inequality and $\overline{V}(0,0) = 0$ actually imply that $\overline{V}(\overline{x}(t''(\varepsilon))) \leq 0$ for any $\varepsilon \in [0, \varepsilon_0) \cap [0, \delta)$. Indeed:

$$\begin{aligned} \overline{V}(\overline{x}(t'')) &= \overline{V}(\overline{x}(t'')) - \overline{V}(0,0) \\ &= \overline{V}(\overline{x}(t'')) - \overline{V}(\overline{x}(0)) \\ &= \int_0^{t''} \frac{\mathrm{d}\overline{V}(\overline{x}(s))}{\mathrm{d}s}\mathrm{d}t \leq 0. \end{aligned}$$

Nevertheless, recalling the *ad absurdum* assumption $\|\overline{x}(t''(\varepsilon))\| = \varepsilon$ for any $\varepsilon \in [0, \varepsilon_0)$ and positive definiteness of the function $\overline{V}$ one easily gets that $\overline{V}(\overline{x}(t''(\varepsilon))) > 0$ for all $\varepsilon \in [0, \delta)$. Selecting any $\varepsilon \in [0, \varepsilon_0) \cap [0, \delta)$ then gives both $\overline{V}(\overline{x}(t''(\varepsilon))) > 0$ and $\overline{V}(\overline{x}(t''(\varepsilon))) \leq 0$, which is the contradiction. ■

Remark 2.1. The interesting question arises whether the HIPSF perturbed by a nonconstant $\omega(t)$ such that $\Omega_{\min} \leq \omega(t) \leq \Omega_{\max}$ with $[\Omega_{\min}, \Omega_{\max}] \subset [-\theta_2/\theta, \theta_2/\theta]$ has the unique global solution starting at the origin. The proof of the uniqueness part of Proposition 2 heavily depends on the assumption that $\omega(t)$ is constant and cannot be adapted even in the case of very slowly varying and smooth $\omega(t)$. Indeed, replacing in $\overline{V}$ the constant Ω_c by a smooth $\omega(t)$ would give an additional term in the derivative of $\overline{V}$ along some solution, namely, the term $\dot{\omega}(t)x_1$. This term is locally sign indefinite and makes the derivative of $\overline{V}$ along some solution locally sign indefinite even for some very small value of $\dot{\omega}(t)$. This is, of course, no proof of nonuniqueness, nevertheless, both Example 2.1 and numerical simulations later on indicate, that there may be solutions starting at the origin and leaving for nonconstant $\omega(t)$. It is fair to point out here frankly, that the full and precise proof of that property is still missing despite some efforts by the authors of the current paper to obtain it.

Though the HIPSF has the discontinuous right-hand side not only at $(0,0)^\top$, but for all $x = (x_1, x_2)^\top \in \mathbb{R}^2$ such that $x_1 = 0$, outside any neighborhood of the origin, the following simpler definition of solutions is sufficient to study the HIPSF.

Definition 2.3. Let $T > 0$ be given. The mapping

$$[0, T] \mapsto \mathbb{R}^2 : x(t) = (x_1(t), x_2(t))^\top, \quad t \in [0, T],$$

is called the trajectory of (7) on $[0, T]$ if $x_1(t)$ is a differentiable function on $[0, T]$, $x_2(t)$ is a continuous piecewise differentiable function on $[0, T]$ and (7) holds for all $t \in [0, T]$ such that $x_1(t) \neq 0$. The HIPSF (7) is called unperturbed for $\omega(t) \equiv 0$, undamped for $k_1 = 0$, damped for $k_1 > 0$ and perturbed for $\omega(t) \neq 0$. The solution of (7) on $[0, T]$ with the initial condition $(x_1^0, x_2^0)^\top$ is its trajectory $(x_1(t), x_2(t))^\top, t \in [0, T]$, such that $x_1(0) = x_1^0, x_2(0) = x_2^0$. The solution $x(t)$ on $[0, T], T > 0$, is called maximal if there does not exist a solution $\overline{x}(t)$ on $[0, T'], T' > T$, such that $x(t) = \overline{x}(t), \forall\, t \in [0, T]$. The solution is called globally defined, if there is no maximal solution on some bounded interval $[0, T]$.

The following proposition was given in [Čelikovský & Lynnyk, 2018b], including an incomplete sketch of its proof. The full proof of this proposition is one of the main theoretical contributions of the current paper. This proposition actually shows that outside any arbitrarily small neighborhood of the origin, every solution exists and is unique not only in the Filippov sense (Definition 2.2), but also in the sense of Definition 2.3.

Proposition 3. *Given that arbitrary* $\varepsilon > 0$, $(x_1^0, x_2^0)^\top \notin \mathcal{B}_{0,\varepsilon}$ *and a piecewise continuous and globally bounded* $\omega(t)$, *then there exist* $T > 0$ *and a unique solution* $(x_1(t), x_2(t))^\top$ *on* $t \in [0, T]$ *with the initial condition* $x_1(0) = x_1^0, x_2(0) = x_2^0$ *of the HIPSF* (7) *in the sense of Definition 2.3. Moreover, this solution is also the unique solution in the Filippov sense on* $[0, T]$ *and it is either globally defined, or there is a finite time* t_f, *such that it exists on* $[0, t_f]$ *and* $(x_1(t_f), x_2(t_f))^\top \in \mathcal{B}_{0,\varepsilon}$.

Proof. The proof of Proposition 3 is based on Lemmas 1–4 formulated and proved below. First, note that, except points where $x_1 = 0$, the local solution in the Filippov sense is the same as the local one in the sense of Definition 2.3. Moreover, due to Lemma 1 and the standard theorem on the existence and the uniqueness of the solution of the differential equation with the Lipschitz right-hand side, the solution of the HIPSF (7) in the sense of Definition 2.3 exists and it is unique for all initial conditions from the set $\{x \in \mathbb{R}^2 \,|\, x_1 \neq 0\}$. Moreover, it exists at least until it stays inside that set. By Lemma 2, there exists a unique local trajectory $\tilde{x}(t)$ of the HIPSF (7) in the sense of Definition 2.3 passing through any point x^c of the set $\{x \in \mathbb{R}^2 \,|\, x_1 = 0, x_2 \neq 0\}$ which is also a solution in the Filippov sense. By Proposition 3 assumption the point x^c belongs to the set $\{x \in \mathbb{R}^2 \,|\, x_1 = 0, x_2 \neq 0\} \backslash \mathcal{B}_{0,\varepsilon}$ and therefore by Lemma 2 with $\bar{\varepsilon} = \varepsilon/2$ the trajectory $\tilde{x}(t)$ takes x^c to the point $\tilde{x}(\bar{t})$ with $\tilde{x}_1(\bar{t}) \neq 0$, $\mathrm{sign}(\tilde{x}_1(\bar{t})) = \mathrm{sign}(\tilde{x}_2(\bar{t}))$ and $|\tilde{x}_2(\bar{t})| > \varepsilon/2$ for some suitable time moment $\bar{t}$. Now, applying Lemma 4 with $\tilde{\varepsilon} = \varepsilon/2$, the next time when the trajectory crosses the set $\{x \in \mathbb{R}^2 \,|\, x_1 = 0, x_2 \neq 0\}$ is not earlier than after time segment having the length $k_1^{-1} \log(K^{-1}k_1\varepsilon/2+1)$. This length does not depend on the particular crossing of the set $\{x \in \mathbb{R}^2 \,|\, x_1 = 0, x_2 \neq 0\}$, as soon as all crossing points stay outside $\mathcal{B}_{0,\varepsilon}$, as assumed in Proposition 3 formulation. This completes the proof. ■

Lemma 1. *The right-hand side of (7) is globally Lipschitz with respect to* $x \in \mathbb{R}^2$ *both on* $\{x \in \mathbb{R}^2 \,|\, x_1 > 0\}$ *and on* $\{x \in \mathbb{R}^2 \,|\, x_1 < 0\}$. *Moreover, the appropriate Lipschitz constants can be in both cases taken as*

$$L := \max\{\sqrt{2k_1^2 + 1}, \sqrt{2}(\theta_1 + \theta_2)\theta^{-1}\}. \quad (13)$$

Proof. Straightforward computations using the first-order Taylor expansion for the right-hand side of (7) and estimate properly all terms of that expansion. ■

Lemma 2. *Given that arbitrary point* $(0, x_2^c)^\top \in \mathbb{R}$, $x_2^c \neq 0$, *time moment* $t_c > 0$ *and* $\bar{\varepsilon} > 0$, *then there exist* $\delta > 0$ *and a unique trajectory* $\tilde{x}(t)$ *of HIPSF (7) in the sense of Definition 2.3 on* $[t_c, t_c + \delta]$ *such that*:

$$\tilde{x}(t_c) = (0, x_2^c)^\top,$$

$$\mathrm{sign}(\tilde{x}_1(t_c + \delta)) = \mathrm{sign}(\tilde{x}_2(t_c + \delta)) = \mathrm{sign}(x_2^c),$$

$$|\tilde{x}_2(t_c + \delta)| \geq \bar{\varepsilon}.$$

Moreover, $\tilde{x}(t), t \in [t_c, t_c + \delta]$, *is also the unique solution of (10), (11), i.e. the solution of (7) in the Filippov sense.*

Proof. Straightforward computations using the first equation of (7) and of Eqs. (10) and (11). ■

Lemma 3. *Let the assumptions of Proposition 3 hold and denote* $\overline{\omega} := \sup_{t\geq 0} |\omega(t)|$. *Let* $x(t)$ *be any trajectory of the HIPSF (7) in the sense of Definition 2.3 such that* $x_1(t) \neq 0$ *for all* $t \in [t', t'']$, $t'' > t' > 0$. *Then for any trajectory* $x(t)$ *on* $[t', t'']$ *it holds that* $\forall\, t \in [t', t'']$:

$$|x_2(t)| \geq |(|x_2(t')| + Kk_1^{-1}) \times \exp(-k_1(t - t')) - Kk_1^{-1}|,$$

$$K := \left(\frac{\theta_1}{\theta} + \frac{\theta_2}{\theta}\right) + \overline{\omega}.$$

Proof. The second equation of (7), which holds by the assumption $x_1(t) \neq 0$ for all $t \in [t', t'']$ on the whole interval $[t', t'']$, gives straightforwardly

$$\forall\, t \in [t', t''] : \dot{x}_2 = \phi(x, t) - k_1 x_2,$$

$$|\phi(x, t)| \leq \left(\frac{\theta_1}{\theta} + \frac{\theta_2}{\theta}\right) + \overline{\omega} = K,$$

$$x_2(t) = \exp(-k_1 t) \times \left(x_2(t') + \int_{t'}^{t} \exp(k_1 s)\phi(x(s), s)\mathrm{d}s\right), \quad \forall\, t \in [t', t''].$$

Using the well-known inequality $|a + b| \geq ||a| - |b||, \forall\, a, b \in \mathbb{R}$, taking the absolute value inside the integral, using $|\phi(x, t)| \leq K$ and calculating the integral of the exponential function give $\forall\, t \in [t', t'']$ that

$$\begin{aligned} |x_2(t)| &\geq \exp(-k_1(t - t')) \times \left| |x_2(t')| - K \int_{t'}^{t} \exp(k_1 s)\mathrm{d}s \right| \\ &= |(|x_2(t')| + Kk_1^{-1}) \times \exp(-k_1(t - t')) - Kk_1^{-1}|, \end{aligned}$$

which completes the proof. ■

Lemma 4. *Let the assumptions and notations of Lemma 3 hold. Let* $x(t)$ *be an arbitrary trajectory of HIPSF (7) in the sense of Definition 2.3 such that for some* $t' \geq 0$, $x_1(t') \neq 0$ *holds*, $|x_2(t')| \geq \tilde{\varepsilon}$, $\mathrm{sign}(x_1(t')) = \mathrm{sign}(x_2(t'))$. *Then we get*

$$x_1(t) \neq 0, \quad x_2(t) \neq 0, \quad \mathrm{sign}(x_1(t)) = \mathrm{sign}(x_2(t)), \quad \forall\, t \in [t', t' + k_1^{-1} \log(K^{-1}k_1\tilde{\varepsilon} + 1)].$$

Proof. First, let us realize that the conditions $x_1(t) \neq 0$, $x_2(t) \neq 0$, $\mathrm{sign}(x_1(t)) = \mathrm{sign}(x_2(t))$ to be proved should hold on any interval $[t', t'']$ where $\forall\, t \in [t', t'']$ and $x_2(t) \neq 0$, $\mathrm{sign}(x_2(t)) = \mathrm{sign}(x_2(t'))$. Indeed, if $x_1(t) \neq 0\ \forall\, t \geq t'$, such a claim is trivial, otherwise, denote $t''' = \inf\{t \in \mathbb{R} \,|\, x_1(t) = 0\}$. Since $x_1(t') \neq 0$, by continuity argument $t''' > t'$ and $x_1(t) \neq 0$, $\mathrm{sign}(x_1(t)) = \mathrm{sign}(x_1(t)')$, $\forall\, t \in [t', t''')$. In particular, the equations of HIPSF (7) hold on the whole interval $[t', t''')$ and therefore

$$x_1(t''') = x_1(t') + \int_{t'}^{t'''} x_2(s)\mathrm{d}s.$$

Obviously, previous equality gives for $x_2(t) \neq 0$, $\mathrm{sign}(x_1(t)) = \mathrm{sign}(x_2(t))$, $t \in [t', t''']$ that $|x_1(t''')| > |x(t')|$. Since $x_1(t') \neq 0$ by Lemma 4 assumption, one has that $x_1(t''') \neq 0$, which contradicts the definition of t'''.

Secondly, applying Lemma 3, one has that

$$\begin{aligned}|x_2(t)| &\geq |(|x_2(t')| + Kk_1^{-1}) \\ &\quad \times \exp(-k_1(t-t')) - Kk_1^{-1}| \\ &= |(\tilde{\varepsilon} + Kk_1^{-1})\exp(-k_1(t-t')) - Kk_1^{-1}|.\end{aligned}$$

Assume that $x_2(t^*) = 0$ for some $t^* > t'$, then

$$\begin{aligned}0 &= |x_2(t^*)| \\ &\geq |(\tilde{\varepsilon} + Kk_1^{-1})\exp(-k_1(t^*-t')) - Kk_1^{-1}| \\ &\Rightarrow \ \exp(-k_1(t^*-t')) = \frac{Kk_1^{-1}}{\tilde{\varepsilon} + Kk_1^{-1}}.\end{aligned}$$

Applying logarithm to both sides of the latter equality gives after straightforward manipulations that

$$t^* = t' + k_1^{-1}\log(K^{-1}k_1\varepsilon + 1).$$

Moreover, for all $t \in [t', t^*]$, we obviously get

$$\begin{aligned}|x_2(t)| &\geq |(\varepsilon + Kk_1^{-1})\exp(-k_1(t-t')) - Kk_1^{-1}| \\ &> 0,\end{aligned}$$

i.e. for all $t \in [t', t' + k_1^{-1}\log(K^{-1}k_1\varepsilon + 1)]$, $x_2(t) \neq 0, \mathrm{sign}(x_2(t)) = \mathrm{sign}(x_2(t'))$. By applying the observation proved at the beginning of this proof, we conclude it. ■

Corollary 2.1. *Let all assumptions and notations of Proposition 3 hold and let $\omega \equiv 0$. Denote the existing solution of (7) in the sense of Definition 2.3 mentioned in the formulation of Proposition 3 as $x(t, x^0)$, $x(0, x^0) = x^0$. Then $x(t, x^0)$ depends continuously on its initial conditions x^0 and $x(t, x^0) = x(t-t', x(t', x^0))$ for all $t > t' > 0$ where the solution exists. Finally, let any $\varepsilon > 0$ be given, then the solution of (7) in the sense of Definition 2.3, $x(t, x^0)$, either exists globally for all $t \geq 0$ or there is some $t_f > 0$ such that $x(t, x^0)$ exists for all $t \in [0, t_f]$ and $x(t_f, x^0) \in \mathcal{B}_{0,\varepsilon}$. Moreover, if $x(t, x^0)$ exists for some $t > t_f$, then $x(t, x^0) \in \mathcal{B}_{0,\varepsilon}$.*

Proof. Continuous dependence on initial conditions follows straightforwardly by the construction of the solution during the proof of Proposition 3. The same observation applies to the second property as the HIPSF with $\omega \equiv 0$ being time invariant.

To prove the last corollary claim, note first that if this claim holds for all $\varepsilon \leq \bar{\varepsilon}$, where $\bar{\varepsilon}$ is some positive real, then it obviously holds for all $\varepsilon > 0$. Next, consider the function $V : \mathbb{R}^2 \mapsto \mathbb{R}$ given by

$$V(x_1, x_2) = \theta_1(\cos x_1 - 1) + \theta_2|\sin x_1| + \frac{\theta x_2^2}{2} \tag{14}$$

and let $x(t)$ be any trajectory of (7). Straightforward computations show that $V(x(t)) : \mathbb{R} \mapsto \mathbb{R}$ is everywhere continuous and differentiable except for isolated time moments and

$$\frac{\mathrm{d}V(x(t))}{\mathrm{d}t} = -\theta k_1 x_2^2 + \theta\omega(t)x_2. \tag{15}$$

As a consequence, due to the corollary assumption $\omega \equiv 0$, $V(x(t)) : \mathbb{R} \mapsto \mathbb{R}$ is a continuous and nonincreasing function of time on any finite time interval. Moreover, $V(0) = 0$ and there obviously exists $\bar{\varepsilon} > 0$ such that $V(x) > 0\ \forall\, x \in \mathcal{B}_{0,\bar{\varepsilon}}\backslash\{0\}$, since $(\partial V/\partial x_1) = -\theta_1 \sin x_1 + \theta_2 \mathrm{sign}(x_1)\cos x_1, x_1 \neq 0$, $(\partial V/\partial x_2) = \theta x_2$. Take any $\varepsilon \in (0, \bar{\varepsilon}]$, then by the mentioned properties of $V : \mathbb{R}^2 \mapsto \mathbb{R}$ there exists $c(\varepsilon) > 0$ and $\delta(c(\varepsilon)) > 0$ such that

$$\mathcal{B}_{0,\delta(c(\varepsilon))} \subset \{x \in \mathbb{R}^2 \,|\, V(x) < c(\varepsilon)\} \cap \mathcal{B}_{0,\bar{\varepsilon}} \subset \mathcal{B}_{0,\varepsilon}. \tag{16}$$

Indeed, the claim related to the right inclusion in (16) follows *ad absurdum* as follows. Assume that it does not hold, then for any $\varepsilon \in (0, \bar{\varepsilon}]$ and any $c > 0$ there exists $\tilde{x} \in \mathcal{B}_{0,\bar{\varepsilon}}, \tilde{x} \notin \mathcal{B}_{0,\varepsilon}$ such that $V(\tilde{x}) < c$. As a consequence, by the continuity of V and the compactness of $\mathcal{B}_{0,\bar{\varepsilon}}\backslash\mathcal{B}_{0,\varepsilon}$ there exists $\overline{x} \in \mathcal{B}_{0,\bar{\varepsilon}}\backslash\mathcal{B}_{0,\varepsilon}$ such that $V(\overline{x}) = 0$. The latter property is the obvious contradiction to the property that $V(x) > 0\ \forall\, x \in \mathcal{B}_{0,\bar{\varepsilon}}\backslash\{0\}$.

The left inclusion in (16) is the direct consequence of the generally adopted definition of the continuity of V at 0 since, due to $V(0) = 0$ and $V(x) > 0$ for $x \neq 0$ around the origin, the set $\{x \in \mathbb{R}^2 \,|\, V(x) < c(\varepsilon)\}$ is the preimage of function V of the open interval $(-c(\varepsilon), c(\varepsilon))$.

Now, to prove the last claim of the corollary note, by Proposition 3 there exists t_f such that the trajectory until t_f and $x(t_f)$ belongs to $\mathcal{B}_{0,\delta(c(\varepsilon))}$. Since $V(x(t))$ is nonincreasing along trajectories of (7), using (16) one has that the trajectory $x(t)$ belongs to $\mathcal{B}_{0,\varepsilon}$ for all $t \geq t_f$ where it exists. ■

Based on the above results, the following proposition can be proved. As a matter of fact, we see that the unperturbed HIPSF is Lyapunov stable and, moreover, if it is damped, it is asymptotically stable as implied by that proposition.

Proposition 4. *Let $k_1 \geq 0, \omega \equiv 0$ and let $x_1^0, x_2^0 \in \mathcal{A}\backslash\{0\}$, where*

$$\mathcal{A} = \{x \in \mathbb{R}^2 \,|\, V(x_1, x_2) < \sqrt{\theta_1^2 + \theta_2^2} - \theta_1 \wedge |x_1| \leq \arctan(\theta_2\theta_1^{-1})\}, \quad (17)$$

V given by (14). If $k_1 = 0$, then there exists a maximal unique solution of (7), $x(t), t \in [0, \infty)$, $x_1(0) = x_1^0, x_2(0) = x_2^0$ in the sense of Definition 2.3. Further, if $k_1 \geq 0$ then $\forall\, \varepsilon > 0\; \exists\, \delta(\varepsilon) > 0$ such that $(x_1^0, x_2^0)^\top \in \mathcal{B}_{0,\delta(\varepsilon)} \Rightarrow x(t) \in \mathcal{B}_{0,\varepsilon}, \forall\, t \geq 0$ for which that solution $x(t)$ with $x_1(0) = x_1^0, x_2(0) = x_2^0$ exists. Finally, assume that $k_1 > 0$, then either $x(t) \to 0$ as $t \to \infty$ or there exists $t_f > 0$ such that $x(t) \to 0$ as $t \to t_f$.

Remark 2.2. Recall, that the trivial trajectory $x(t) \equiv 0$ is not the solution of (7) in the sense of Definition 2.3, therefore the last statement of Proposition 4 cannot be reduced to $x(t) \to 0$ as $t \to \infty$ only. In the sequel, we will shortly refer these two situations mentioned at the end of Proposition 4 as *asymptotical stability* and *finite-time stability*, where appropriate. Note, that for the HIPSF and its equilibrium at the origin neither of these notions is stronger than the other one.

Proof. Proposition 3 and Corollary 2.1 provide in a sense an easy way to avoid the study of a peculiar behavior of a trajectory approaching the equilibrium at the origin, which is, as already noted, properly defined only in the Filippov sense. Indeed, the real number $\varepsilon > 0$ in Corollary 2.1 is arbitrary, so that either the investigated trajectory enters any neighborhood of the origin and stays within there, which is exactly the claim to be proved, or for all $t \geq 0$ it exists outside some neighborhood of the origin. The latter means that such a trajectory is well defined in the sense of Definition 2.3 and the Lyapunov-like function V given by (14) can be easily used to produce a contradiction, despite its piecewise differentiability only.

Last but not least, the issue to be solved during the proof just illustrated is as follows. The Lyapunov-like function V given by (14) does not possess the negative definite time derivative along the trajectory, so that some standard manipulations that mimic the well-known LaSalle principle are needed as well. As a matter of fact, one can use the LaSalle principle thanks to Corollary 2.1.

To start the above plan in detail, realize first that the set $\mathcal{A}$ given by (17) is bounded. Indeed, the first term in V is non-negative for all x_1 such that $|x_1| \leq 2\arctan(\theta_2\theta_1^{-1})$, since

$$\begin{aligned}
&\theta_1(\cos x_1 - 1) + \theta_2|\sin x_1| \\
&\quad = -2\theta_1 \sin^2\left(\frac{x_1}{2}\right) + 2\theta_2 \left|\sin\left(\frac{x_1}{2}\right)\right| \left|\cos\left(\frac{x_1}{2}\right)\right| \\
&\quad = 2\theta_2 \left|\cos\left(\frac{x_1}{2}\right)\right| \left|\sin\left(\frac{x_1}{2}\right)\right| \\
&\qquad \times \left(1 - \theta_2^{-1}\theta_1 \left|\tan\left(\frac{x_1}{2}\right)\right|\right) \\
&\quad \geq 0 \quad\Leftrightarrow\quad |x_1| \leq 2\arctan(\theta_2\theta_1^{-1}).
\end{aligned}$$

As a consequence, it obviously holds that

$$\mathcal{A} \subset \left\{x = (x_1, x_2)^\top \in \mathbb{R}^2 : \frac{\theta x_2^2}{2} < \sqrt{\theta_1^2 + \theta_2^2} - \theta_1, |x_1| \leq \arctan(\theta_2\theta_1^{-1})\right\},$$

i.e. $\mathcal{A}$ is the subset of the bounded set.

Next, using the function V given by (14), define the following family of the nested sets

$$V_c := \{x \in \mathcal{A} : V(x) \leq c\}, \quad c \in (0, \sqrt{\theta_1^2 + \theta_2^2} - \theta_1),$$

$$c_1 \leq c_2 \;\Rightarrow\; V_{c_1} \subset V_{c_2}.$$

Further, for all $x = (x_1, x_2)^\top \in \mathcal{A}$ the function $V(x)$ given by (14) is obviously continuous, positive definite with $V(0) = 0$ and continuously differentiable for $x_1 \neq 0$. Moreover, the straightforward computations show that its gradient $V_x = (V_{x_1}, V_{x_2})$ satisfies that

$$\begin{aligned}
&V_{x_1}x_1 + V_{x_2}x_2 \\
&\quad = |x_1|\cos(x_1)(\theta_2 - \theta_1\tan(|x_1|)) + \theta x_2^2 \\
&\quad > 0, \quad \forall\, x \in \mathcal{A}\backslash\{x \in \mathbb{R}^2 : x_1 = 0\}.
\end{aligned}$$

As a consequence, by Taylor expansion, $\forall\, \overline{x} \in \mathcal{A}\backslash\{x \in \mathbb{R}^2 : x_1 = 0\}$, $\forall\, c \in (0, \sqrt{\theta_1^2 + \theta_2^2} - \theta_1)$ such that $V(\overline{x}) = c$ and $\forall\, \epsilon > 0$, there exists $\tilde{x} \in \mathcal{A}$, such that $\|\tilde{x} - \overline{x}\| < \epsilon$ and $V(\tilde{x}) > c$. In other words, denoting by ∂V_c the boundary of V_c, we get

$$\forall\, c \in (0, \sqrt{\theta_1^2 + \theta_2^2} - \theta_1),$$

$$\partial V_c = \{x \in \mathcal{A} : V(x) = c\},$$

since any neighborhood of $x \in \partial V_c\backslash\{x \in \mathbb{R}^2 : x_1 = 0\}$ contains a point not belonging to V_c. Moreover, points $(0, \pm\sqrt{2c/\theta})^\top \in V_c$ are clearly the boundary ones of V_c as well if $c \in (0, \sqrt{\theta_1^2 + \theta_2^2} - \theta_1)$. Summarizing, for all $x \in \mathcal{A}$ the equality $V(x) = c$ implies that $x \in \partial V_c$. Finally, by continuity of V, all points of the set $\{x \in \mathcal{A} : V(x) < c\}$ are the interior points of V_c and therefore $x \in \partial V_c$ implies $V(x) = c$.

The above proved property that $\partial V_c = \{x \in \mathcal{A} : V(x) = c\}, \forall\, c \in (0, \sqrt{\theta_1^2 + \theta_2^2} - \theta_1)$ implies that $\partial V_{c_1} \cap \partial V_{c_2} = \emptyset\ \forall\, c_1, c_2 \in (0, \sqrt{\theta_1^2 + \theta_2^2} - \theta_1), c_1 < c_2$ and therefore also that $V_{c_1} \subset \operatorname{int} V_{c_2}\ \forall\, c_1, c_2 \in (0, \sqrt{\theta_1^2 + \theta_2^2} - \theta_1), c_1 < c_2$. As a consequence, the origin $0 \in \operatorname{int} V_c\ \forall\, c \in (0, \sqrt{\theta_1^2 + \theta_2^2} - \theta_1)$.

Now, consider any trajectory $x(t) = (x_1(t), x_2(t))^\top$ of the HIPSF (7). Straightforward computations show that for all t where $x(t)$ exists, the composed map $V(x(t))$ is a continuous function. Moreover, if $x_1(t) \neq 0$, then it holds that

$$\frac{\mathrm{d}V(x(t))}{\mathrm{d}t} = -\theta k_1 x_2^2 + \theta\omega(t)x_2, \quad \forall\, x_1 \neq 0,\ \ x_2 \in \mathbb{R}. \tag{18}$$

The equality (18) implies that for the unperturbed undamped case (i.e. $\omega(t) \equiv 0, k_1 = 0$) the function V is constant along trajectories when $x_1(t) \neq 0$. Note that $\forall\, r > 0$, the set $\{x \in \mathbb{R}^2 : x_1 = 0\} \cap \mathcal{B}_{0,r}$ is not invariant along trajectories of (7) in the sense of Definition 2.3 existing due to Proposition 3. This implies easily the first claim of Proposition 4. Indeed, take any $x_1^0, x_2^0 \in \mathcal{A}\backslash\{0\}$, and let $x(t)$ be the solution of (7) in the sense of Definition 2.3 with $x_1(0) = x_1^0, x_2(0) = x_2^0$. Then $V(x(t)) \equiv V(x(0)) > 0$ and by the above proved properties of V the solution $x(t)$ stays outside some fixed neighborhood of the origin, i.e. due to Proposition 3, it exists for all $t \geq 0$.

The second claim of Proposition 4 can be proved as follows. Let $\varepsilon > 0$ be given, then by the continuity of V at the origin there exists $c(\varepsilon) > 0$ such that $V_{c(\varepsilon)} \subset \mathcal{B}_{0,\varepsilon}$. Previously, we proved that the set $V_{c(\varepsilon)}, c(\varepsilon) > 0$, contains the neighborhood of the origin, i.e. there exists $\delta(c(\varepsilon)) > 0$ such that $\mathcal{B}_{0,\delta(c(\varepsilon))} \subset V_{c(\varepsilon)}$. Take $(x_1^0, x_2^0)^\top \in \mathcal{B}_{0,\delta(c(\varepsilon))}$, then the solution of (7) in the sense of Definition 2.3 with $x_1(0) = x_1^0, x_2(0) = x_2^0$ satisfies by (18) and by $\omega(t) \equiv 0$ that $V(x(t)) \leq V(x(0)) \leq c(\varepsilon), \forall\, t \geq 0$ and therefore $x(t) \in V_{c(\varepsilon)} \subset \mathcal{B}_{0,\varepsilon}$ for all $t \geq 0$. This completes the proof of the second claim.

To prove the last claim of Proposition 4, assume its contrary which (using Corollary 2.1) is clearly equivalent to the existence of some $\epsilon > 0$ and a trajectory $x(t)$ which stays outside the ϵ-neighborhood of the origin $\forall\, t \geq 0$. By Proposition 3, the trajectory $x(t)$ exists $\forall\, t \geq 0$, by (15) along $x(t)$ it holds $\dot{V} = -k_1 x_2^2,\ k_1 > 0$. Therefore $V(x(t)), t \geq 0$, is a nonincreasing continuous function and its time derivative is uniformly continuous as $\dot{V} = -k_1 x_2^2$, $k_1 > 0$ and $x_2(t),\ t \geq 0$, is bounded by the previously proved properties. Moreover, as $V(x(t))$ is bounded from below, it has finite limit as $t \to \infty$. Since its time derivative is uniformly continuous on $[0, \infty)$, by the well-known property, known also as the Barbalat lemma, $\dot{V}(x(t)) \to 0$ as $t \to \infty$ and therefore $x(t) \to \{x \in \mathbb{R}^2 : x_2 = 0\}\backslash\mathcal{B}_{0,\epsilon}$. Finally, Corollary 2.1 shows that the well-known basic property of the ω-limit set being an invariant set holds for HIPSF as well, as its flow is transitive and continuous on every finite time interval. This means that the set $\{x \in \mathbb{R}^2 : x_2 = 0\}\backslash\mathcal{B}_{0,\epsilon}$ should contain the invariant subset, which is a clear contradiction. Indeed, due to the second equation of (7), $\forall\, r > 0$ holds for the set $\{x \in \mathbb{R}^2 : x_1 = 0\} \cap \mathcal{B}_{0,r}$ being not invariant along trajectories of (7) in the sense of Definition 2.3 existing due to Proposition 3. ■

Remark 2.3. The function V given by (14) can be also used to compute separatrices forming the boundary of stable region of the unperturbed undamped hybrid inverted pendulum. Indeed, these separatrices clearly form a level set $V(x) = c_{\mathrm{sep}} = V(x_1^{E_1}) = V(x_1^{E_2})$. By (9), we get

$$\begin{aligned} c_{\mathrm{sep}} &= \theta_2|\sin x_1^{E_{1,2}}| + \theta_1(\cos x_1^{E_{1,2}} - 1) \\ &= \sqrt{\theta_1^2 + \theta_2^2} - \theta_1 \end{aligned} \tag{19}$$

and the separatrices are therefore given by the pair of curves

$$x_2 = \pm\sqrt{2\theta^{-1}(\sqrt{\theta_1^2 + \theta_2^2} - \theta_2|\sin x_1| - \theta_1\cos x_1)}, \tag{20}$$

where $x_1 \in [x_1^{E_2}, x_1^{E_1}]$, cf. Fig. 3. Furthermore, for the case $k_1 > 0$, $\omega(t) \equiv 0$, the previously mentioned region may be considered as the inner estimate of the region of attraction of the equilibrium at the origin, where the attraction is meant either in the sense of asymptotical stability, or finite-time stability.

Remark 2.4. Proposition 4 can be generalized straightforwardly from the case $\omega \equiv 0$ to the case $\omega(t) \equiv \Omega_c$, where $\Omega_c \in [-\theta_2/\theta, \theta_2/\theta]$. Indeed, in this case by Proposition 2 the origin is the equilibrium in the Filippov sense and the corresponding trivial solution is the unique solution starting at the origin.

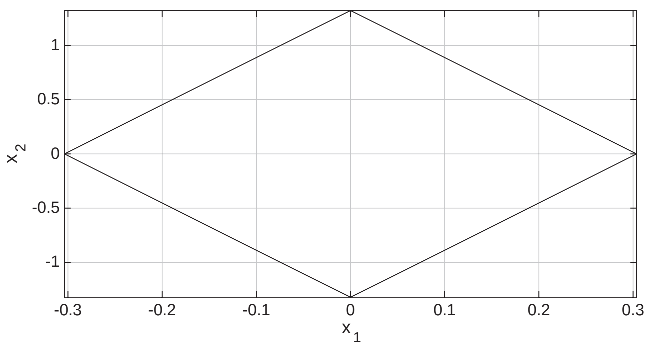

Fig. 3. Separatrices (19) and (20) for $\theta_1 = 3.4433$, $\theta_2 = 1.0791$, $\theta = 0.1891$. $x_1^{E_1} = 0.3037$, $x_2^{E_1} = 0$, $x_1^{E_2} = -0.3037$, $x_2^{E_2} = 0$.

Moreover, consider Lyapunov function $\overline{V}$ introduced during the proof of Proposition 2, namely:

$$\overline{V}(x_1, x_2) = \theta_1(\cos x_1 - 1) + \theta_2|\sin x_1| - \theta\Omega_c x_1 + \frac{\theta x_2^2}{2}.$$

Recall, that it was shown during the proof of Proposition 2 that, if and only if $\Omega \in [-\theta_2/\theta, \theta_2/\theta]$, there exists $\delta > 0$ such that $\overline{V}(0) = 0$ and $V(x) > 0\ \forall\, x \in \mathcal{B}_{0,\delta}, x \neq 0$. Furthermore, it was also shown during the proof of Proposition 2 that

$$\frac{\mathrm{d}\overline{V}(x(t))}{\mathrm{d}t} = -\theta k_1 x_2^2.$$

In such a way, even in the case $\omega(t) \equiv \Omega_c$, $\Omega \in [-\theta_2/\theta, \theta_2/\theta]$, one can conclude as in the proof of Proposition 4 that the HIPSF (7) is locally Lyapunov stable for $k_1 = 0$ and locally asymptotically, or finite-time, stable for $k_1 > 0$. The basin of attraction would be modified by that lateral force as the other classical saddle point equilibria are shifted, further analysis of the region of attraction is omitted for brevity. Such a phenomenon is exceptional and it is due to the hybrid nature of the HIP and the fact that the equilibrium at the origin exists only in the Filippov sense. Indeed, forcing e.g. the classical pendulum by constant external force would just shift the equilibrium from downward position to a deviated one. Note the following straightforward physical interpretation of the above hybrid phenomenon: if the lateral force is constant and not exceeding certain threshold, the HIP movement in a close proximity of the double support equilibrium is not destabilized by that lateral force. Nevertheless, numerical simulations presented later show that a time-varying $\omega(t)$ belonging at all time to $[-\theta_2/\theta, \theta_2/\theta]$ can generate a trajectory of the HIPSF starting arbitrarily close to the origin but always leaving some fixed small ball centered at the origin.

3. Topological Linearizability of the HIPSF Dynamics

First, some facts from dynamical systems theory are repeated for the sake of the self-complete exposition.

Definition 3.1. Consider the following time invariant dynamical systems each having its own state space variable, denoted x and z, respectively, and its own time variable, denoted t and τ, respectively:

$$\begin{aligned}\frac{\mathrm{d}x}{\mathrm{d}t} &= f(x(t)), \quad x \in \mathbb{R}^n,\\ \frac{\mathrm{d}z}{\mathrm{d}\tau} &= g(z(\tau)), \quad z \in \mathbb{R}^n.\end{aligned} \tag{21}$$

Let $\Omega^x \subset \mathbb{R}^n$ and $\Omega^z \subset \mathbb{R}^n$ be some regions of $\mathbb{R}^n$. Assume that f and h are such that the unique Filippov solutions $x(t, x_0), z(\tau, z_0)$, $x(0, x_0) = x_0$, $z(0, z_0) = z_0$ exist for all initial conditions $x_0 \in \Omega^x \subset \mathbb{R}^n$, $z_0 \in \Omega^z \subset \mathbb{R}^n$ and all times $t \in \mathbb{R}$, $\tau \in \mathbb{R}$, and $x(t, x_0) \in \Omega^x\ \forall\, t \in \mathbb{R}, z(\tau, z_0) \in \Omega^x\ \forall\, \tau \in \mathbb{R}$. Systems (21) are called mutually topologically equivalent on regions Ω^x, Ω^z if there exists homeomorphism between $\mathbb{R} \times \Omega^x$ and $\mathbb{R} \times \Omega^z$ of the form

$$\begin{bmatrix}\tau(t, x)\\ \mathcal{T}(x)\end{bmatrix} : \mathbb{R} \times \Omega^x \mapsto \mathbb{R} \times \Omega^z, \tag{22}$$

such that for all $x_0 \in \Omega^x$ and for all $t \in \mathbb{R}$, we get

$$z(\tau(t, x_0), \mathcal{T}(x_0)) \equiv \mathcal{T}(x(t, x_0)), \quad \tau(0, x_0) = 0. \tag{23}$$

If one of those systems is linear, the other one is called *topologically linearizable* in the respective region.

Recall that the brief notation $\dot{x}$ is used for the derivative with respect to the original ("real") time t, i.e. $\dot{x} := \mathrm{d}x/\mathrm{d}t$. For brevity, Definition 3.1 considers only the systems where solutions exist and are unique for all time moments which is sufficient for purposes of the current paper. As a matter of fact, the relation (23) implies certain property of the dependence of the new time τ on the original time t. It is given by the following:

Lemma 5. *Let $\tau(t, x)$ be such that it provides topological equivalence between time invariant systems (21) in the sense of Definition 3.1. Then $\forall\, x_0 \in \Omega^x$ and $\forall\, t \in \mathbb{R}, \forall\, t' \in \mathbb{R}, t > t'$ hold,*

$$\tau(t, x_0) = \tau(t - t', x(t', x_0)) + \tau(t', x_0). \quad (24)$$

Proof. A straightforward consequence of the well-known group property of solutions, i.e. $x(0, x_0) = x_0, z(0, z_0) = z_0$ and $x(t - t', x(t', x_0)) = x(t, x_0)$, $\forall\, t \geq t', \forall\, x_0 \in \Omega^x$ and $z(\tau - \tau', z(\tau', z_0)) = z(\tau, z_0)$, $\forall\, \tau \geq \tau', \forall\, z_0 \in \Omega^z$. ■

Proposition 5. *Consider time invariant dynamical systems (21) having each its own state space variable, denoted x and z, respectively, and its own time variable, denoted t and τ, respectively. Let $\Omega^x \subset \mathbb{R}^n$ and $\Omega^z \subset \mathbb{R}^n$ be both forward and backward invariant compact sets of the respective system. Assume that f and g are such that the unique Filippov solutions $x(t, x_0), z(\tau, z_0)$, $x(0, x_0) = x_0$, $z(0, z_0) = z_0$ exist for all initial conditions $x_0 \in \Omega^x \subset \mathbb{R}^n$, $z_0 \in \Omega^z \subset \mathbb{R}^n$ and all times $t \in \mathbb{R}$, $\tau \in \mathbb{R}$. Then these systems are mutually topologically equivalent with the mapping (22) being diffeomorphism if and only if there exists diffeormorphism $\mathcal{D}(x) : \Omega^x \mapsto \Omega^z$ and a smooth function $s(x) : \Omega^x \mapsto (0, \infty)$, such that*

$$g(\mathcal{D}(x)) = s(x)\frac{\partial \mathcal{D}}{\partial x}(x) f(x). \quad (25)$$

Proof. **"Only if" Part:** Assume that the mappings $\mathcal{T}$ and $\tau(t, x)$ are smooth. Chain rule and (21) give

$$g(z(\tau)) = \frac{\mathrm{d}z}{\mathrm{d}\tau} = \frac{\partial \mathcal{T}}{\partial x}\frac{\mathrm{d}x}{\mathrm{d}\tau} = \frac{\partial \mathcal{T}}{\partial x}\frac{\mathrm{d}x}{\mathrm{d}t}\left[\frac{\mathrm{d}\tau}{\mathrm{d}t}\right]^{-1} = \left[\frac{\mathrm{d}\tau}{\mathrm{d}t}\right]^{-1}\frac{\partial \mathcal{T}}{\partial x} f(x(t)).$$

In other words, recalling that $z = \mathcal{T}(x)$, one has

$$g(\mathcal{T}(x(t))) = \left[\frac{\mathrm{d}\tau}{\mathrm{d}t}\right]^{-1}\frac{\partial \mathcal{T}}{\partial x}(x(t)) f(x(t)).$$

Differentiating (24) given by Lemma 5 with respect to t and then substituting $t' = t$ one has

$$\frac{\mathrm{d}\tau}{\mathrm{d}t}(t, x_0) = \frac{\partial \tau}{\partial t}(0, x(t, x_0)), \quad \forall\, t \in \mathbb{R},\ \forall\, x_0 \in \Omega^x.$$

Denoting $\mathcal{D} := \mathcal{T}$ and $s(x) := [\frac{\partial \tau}{\partial t}(0, x)]^{-1}$ gives

$$g(\mathcal{D}(x)) = s(x)\frac{\partial \mathcal{D}}{\partial x}(x) f(x).$$

Realize that by the proposition formulation $\tau(t, x_0)$ should be smooth one-to-one map having a smooth inverse for all x_0 and therefore $s(x_0) > 0$ for all x_0 from Ω^x. This completes the proof of the "only if" part.

"If" Part: Take $\mathcal{T}(x) := \mathcal{D}$ and

$$\tau(t, x_0) := \int_0^t s^{-1}(x(s, x_0))\mathrm{d}s, \quad (26)$$

where $x(t, x_0)$ stands for the solution of $\mathrm{d}x/\mathrm{d}t = f(x)$ with $x(0, x_0) = 0$. Since $s(x) > 0$ and Ω^x is the compact set by the proposition formulation, there exists some $\delta > 0$ such that $s(x) > \delta\ \forall\, x \in \Omega^x$. Moreover, recall that by the proposition formulation $x(t, x_0) \in \Omega^x\ \forall\, t \in \mathbb{R}$. As a consequence, (26) defines for every $x_0 \in \Omega^x$ a smooth one-to-one map of $\mathbb{R}$ onto itself. Indeed, by the elementary properties of the integral applied to (26), the function $\tau(t, x_0)$ is continuous, growing and $\lim_{t\to\pm\infty} \tau(t, x_0) = \pm\infty$. The straightforward computations then show that equalities in (23) hold. ■

In the sequel, the function $s(x)$ in (25) will be called the *time scaling*. Topological equivalence preserves qualitative features of the dynamical systems and therefore it is often used for their classification. In particular, topological equivalence maps orbits onto orbits preserving the sense of the time evolution of the trajectories inside these orbits. The qualitative structure of the HIPSF (7) might be better understood realizing that it is actually topologically equivalent to the linear oscillator.

Proposition 5 provides a more constructive way to study the topological equivalence when all maps are diffeomorphisms. Nevertheless, the nondiffeomorphical (i.e. homeomorphic only) case is more useful. In some cases one can look for some almost everywhere diffeomorphical map $\mathcal{T}$ and for some scaling function $s(x)$ being almost everywhere positive, differentiable and bounded, then try to prove the homeomorphic properties required by Definition 3.1 via some extra *ad hoc* analysis. As a matter of fact, such an idea will be used when proving topological linearizability of the HIPSF (7) postulated by the following proposition.

Proposition 6. *The unperturbed and undamped HIPSF (7) is topologically linearizable on the* *region*[1]:

$$\Omega^x = \left\{x \in \mathbb{R}^2 : \theta_2|\sin x_1| + \theta_1 \cos x_1 + \frac{\theta x_2^2}{2} < \sqrt{\theta_1^2 + \theta_2^2} \wedge |x_1| \le \arctan(\theta_2\theta_1^{-1})\right\}. \tag{27}$$

More specifically, the unperturbed and undamped HIPSF (7) is topologically equivalent on bounded region Ω^x given by (27) to the linear harmonic oscillator on bounded region $\Omega^z \subset \mathbb{R}^2$

$$\frac{\mathrm{d}z_1}{\mathrm{d}\tau} = z_2, \quad \frac{\mathrm{d}z_2}{\mathrm{d}\tau} = -z_1, \quad z = (z_1, z_2)^\top \in \Omega^z, \tag{28}$$

$$\Omega^z = \{z = (z_1, z_2)^\top \in \mathbb{R}^2 : z_1^2 + z_2^2 \le 2\theta^{-1}\sqrt{\theta_1^2 + \theta_2^2} - 2\theta^{-1}\theta_1\}. \tag{29}$$

Proof. Consider the following map acting from Ω^x to Ω^z:

$$\begin{aligned} z_1 &= \mathrm{sign}(x_1)\sqrt{2\theta^{-1}\theta_1(\cos x_1 - 1) + 2\theta^{-1}\theta_2|\sin x_1|} \\ &= 2\sin\left(\frac{x_1}{2}\right)\sqrt{\frac{\theta_2 - \theta_1 \tan\left(\frac{x_1}{2}\right)}{\theta \tan\left(\frac{x_1}{2}\right)}}, \\ z_2 &= x_2. \end{aligned} \tag{30}$$

Straightforward computations using (30) give that

$$\begin{aligned} z_1^2 &= 2\theta^{-1}(\theta_1(\cos x_1 - 1) + \theta_2|\sin x_1|), \\ z_2^2 &= x_2^2 \;\Rightarrow\; z_1^2 + z_2^2 \\ &= 2\theta^{-1}\left(\theta_1(\cos x_1 - 1) + \theta_2|\sin x_1| + \frac{\theta x_2^2}{2}\right). \end{aligned}$$

As a consequence, (30) maps Ω^x are given by (27) onto Ω^z as given by (29). Later on, a continuous inversion of (30) at any $z = (z_1, z_2)^\top \in \Omega^z$ will be computed explicitly, showing thereby that the map (30) is a homeomorphism of Ω^x and Ω^z. Further, introduce a new time variable τ via the following time scaling

$$\begin{aligned} \frac{\mathrm{d}\tau}{\mathrm{d}t} = s(x_1) &:= \frac{-\theta_1|\sin x_1| + \theta_2 \cos x_1}{\theta|z_1|} \\ &= \frac{-\theta_1|\sin x_1| + \theta_2 \cos x_1}{\sqrt{2\theta\theta_1(\cos x_1 - 1) + 2\theta\theta_2|\sin x_1|}}. \end{aligned} \tag{31}$$

It will also be proved later on that (31) defines $\tau(t, x)$ depending on t, x in a way required by Definition 3.1. Note, that the time scaling $s(x_1)$ is the well-defined and smooth one only for all $x = (x_1, x_2)^\top \in \Omega^x$, such that $x_1 \neq 0$, moreover it is unbounded close to the set where $x_1 = 0$ (preimage of the set where $z_1 = 0$). As a matter of fact, function $(s(x_1))^{-1}$ is smooth everywhere, but $(s(x_1))^{-1} = 0$ for all $x = (x_1, x_2)^\top \in \Omega^x$, such that $x_1 = 0$. In such a way, the smooth equivalence is excluded by Proposition 5 and some extra efforts are required to show the topological equivalence.

Before doing so, let us show that the transformations (30), (31) "formally" convert HIPSF (7) into the linear harmonic oscillator (28). The homeomorphism (30) is also smooth except for the set where $x_1 = 0$ (preimage of the set where $z_1 = 0$), namely:

$$\frac{\partial z_1}{\partial x_1} = \frac{-\theta_1|\sin x_1| + \theta_2 \cos x_1}{\theta|z_1|}, \quad \frac{\partial z_2}{\partial x_2} = 1.$$

Straightforward computations using the HIPSF equations (7) and the chain rule show that the transformation (30) converts the HIPSF (7) to

$$\frac{\mathrm{d}z_1}{\mathrm{d}t} = s(x_1)z_2, \quad \frac{\mathrm{d}z_2}{\mathrm{d}t} = -s(x_1)z_1.$$

Moreover, note that

$$\frac{\mathrm{d}z}{\mathrm{d}\tau} = \frac{\mathrm{d}z}{\mathrm{d}t}\frac{\mathrm{d}t}{\mathrm{d}\tau} = \frac{\mathrm{d}z}{\mathrm{d}t}\frac{1}{s(x_1)}, \quad z := (z_1, z_2)^\top,$$

giving for all $x \in \mathbb{R}^2$, such that $x_1 \neq 0$, and thereby also for all $z \in \mathbb{R}$ such that $z_1 \neq 0$:

$$\frac{\mathrm{d}z_1}{\mathrm{d}\tau} = z_2, \quad \frac{\mathrm{d}z_2}{\mathrm{d}\tau} = -z_1.$$

Now, let us show that (30), (31) define topological equivalence. To do so, let us first invert the homeomorphism (30). Taking in (30) square power of z_1

[1]Recall, that $\pm\arctan(\theta_2\theta_1^{-1})$ are the lateral equilibria of the HIPSF (7) and therefore by $|x_1| \le \arctan(\theta_2\theta_1^{-1})$ the set Ω^x is the subset of $\{x \in \mathbb{R}^2 : \theta_2|\sin x_1| + \theta_1 \cos x_1 + \theta x_2^2/2 < \sqrt{\theta_1^2 + \theta_2^2}\}$ being the area inside the separatrices shown in Fig. 3.

and some straightforward manipulations, we get

$$\frac{\theta z_1^2}{2} + \theta_1 = \theta_1 \cos x_1 + \theta_2 |\sin x_1|$$
$$= \frac{\theta_1(1-r^2) + 2\theta_2 r}{1+r^2}, \quad r := \left|\tan \frac{x_1}{2}\right|.$$

Further straightforward manipulations give a quadratic equation in r and solving it gives

$$r = \frac{2\theta_2 \pm \sqrt{4\theta_2^2 - \theta z_1^2(\theta z_1^2 + 4\theta_1)}}{\theta z_1^2 + 4\theta_1}. \tag{32}$$

Since r is the substitution variable for $|\tan \frac{x_1}{2}|$ and $x_1 = 0$ if and only if $z_1 = 0$, only the branch giving $r = 0$ for $z_1 = 0$ is acceptable, i.e. the one with $\pm$ replaced by minus. Finally, recalling the relation lost while taking the square power of z_1, namely, $\mathrm{sign}(x_1) = \mathrm{sign}(z_1)$, gives the following inverse transformation

$$x_1 = 2\,\mathrm{sign}(z_1) \arctan \frac{2\theta_2 - \sqrt{4\theta_2^2 - \theta z_1^2(\theta z_1^2 + 4\theta_1)}}{\theta z_1^2 + 4\theta_1},$$
$$z_1^2 < 2\theta^{-1}\left(\sqrt{\theta_1^2 + \theta_2^2} - \theta_1\right). \tag{33}$$

Note, that (by some straightforward computations) the range of z_2 given in (33) holds if and only if the expression under the square root in (33) is positive. At the same time, it is clear that for all $z = (z_1, z_2)^\top \in \Omega^z$ given by (29) the component z_2 is within the range of z_2 given in (33). In such a way, the map $z \mapsto x$ defined by the equality (33) together with $x_2 = z_2$ is well-defined for all $z = (z_1, z_2)^\top \in \Omega^z$. Just to double check that both the map (30) and its inverse (33) give one-to-one correspondence between Ω^x given by (27) and Ω^z given by (29), let us compute in (33) the value of $x = (x_1, x_2)^\top$ at boundary points of the range of $z = (z_1, z_2)^\top$ in (33). Recall that these boundary points correspond to the case where square root in (33) is zero and $\theta z_1^2 = 2(\sqrt{\theta_1^2 + \theta_2^2} - \theta_1)$, i.e. the values of $x = (x_1, x_2)^\top$ at these boundary points are equal to:

$$\pm 2 \arctan \frac{\theta_2}{\sqrt{\theta_1^2 + \theta_2^2} + \theta_1} = \pm \arctan\left(\frac{\theta_2}{\theta_1}\right),$$

where the last equality is due to some straightforward manipulations based on the well-known goniometric relation between $\tan x_1$ and $\tan(x_1/2)$. Note, that the obtained boundary values for x_1 are exactly those of (27) for $x_2 = 0$.

Last, but not least, note, that the map (33) is obviously continuous at all $z = (z_1, z_2)^\top \in \Omega^z$. Summarizing, the continuous map (30) and its continuous inverse (33) give one-to-one correspondence between Ω^x given by (27) and Ω^z given by (29), as required by Definition 3.1.

It remains to prove the required properties of the map $\tau(t, x)$. Using the above substitution $r = |\tan \frac{x_1}{2}|$, $|\sin x_1| = 2r(1 + r^2)^{-1}$, $\cos x_1 = (1 + r^2)(1 + r^2)^{-1}$ hold and substituting from (32) gives:

$$|\sin x_1| = \frac{2\left(2\theta_2 - \sqrt{4\theta_2^2 - \theta z_1^2(\theta z_1^2 + 4\theta_1)}\right)(\theta z_1^2 + 4\theta_1)}{(\theta z_1^2 + 4\theta_1)^2 + \left(2\theta_2 - \sqrt{4\theta_2^2 - \theta z_1^2(\theta z_1^2 + 4\theta_1)}\right)^2}, \tag{34}$$

$$\cos x_1 = \frac{(\theta z_1^2 + 4\theta_1)^2 - \left(2\theta_2 - \sqrt{4\theta_2^2 - \theta z_1^2(\theta z_1^2 + 4\theta_1)}\right)^2}{(\theta z_1^2 + 4\theta_1)^2 + \left(2\theta_2 - \sqrt{4\theta_2^2 - \theta z_1^2(\theta z_1^2 + 4\theta_1)}\right)^2}. \tag{35}$$

Using (34), (35), the scaling factor (31) converted to z-coordinates, denoted as $\bar{s}(z_1)$, takes the form

$$\bar{s}(z_1) = \frac{\theta_2\left((\theta z_1^2 + 4\theta_1)^2 - \left(2\theta_2 - \sqrt{4\theta_2^2 - \theta z_1^2(\theta z_1^2 + 4\theta_1)}\right)^2 - 2\theta_1\left(2\theta_2 - \sqrt{4\theta_2^2 - \theta z_1^2(\theta z_1^2 + 4\theta_1)}\right)(\theta z_1^2 + 4\theta_1)\right)}{\theta |z_1| \left((\theta z_1^2 + 4\theta_1)^2 + \left(2\theta_2 - \sqrt{4\theta_2^2 - \theta z_1^2(\theta z_1^2 + 4\theta_1)}\right)^2\right)}. \tag{36}$$

Recall, that

$$\frac{d\tau}{dt} = s(x_1) = \bar{s}(z_1) \quad \Rightarrow \quad \frac{dt}{d\tau} = \frac{1}{\bar{s}(z_1)}, \tag{37}$$

and realize that $z_1(\tau)$ is the first component of the solution of the linear oscillator (28) in time τ, i.e.

$$z_1(\tau) = z_1(0) \cos \tau + z_2(0) \sin \tau.$$

In such a way, the relation between times t and τ is as follows

$$t(\tau, z) = \int_0^\tau \frac{d\alpha}{\bar{s}(z_1 \cos \alpha + z_2 \sin \alpha)}, \quad z \in \Omega^z, \quad \tau \in \mathbb{R}, \tag{38}$$

where $\bar{s}$ is given by (36). Realize, that $\bar{s}(z_1)^{-1}$ is continuous and bounded for all $z = (z_1, z_2)^\top \in \Omega^z$ and $\bar{s}(z_1)^{-1} = 0$ if and only if $z_1 = 0$. Moreover, Ω^z given by (29) is the interior of a circle and therefore it holds that $z = (z_1, z_2)^\top \in \Omega^z \Rightarrow z_1 \cos\alpha + z_2 \sin\alpha \in \Omega^z \ \forall\, \alpha \in \mathbb{R}$. Summarizing, the function integrated inside the integral in (38) is a continuous and non-negative function of α, it is strictly positive $\forall\, \alpha \in \mathbb{R}$ such that $z_1 \cos\alpha + z_2 \sin\alpha \neq 0$ and it is zero when $z_1 \cos\alpha + z_2 \sin\alpha = 0$. In such a way, zeroes are isolated, as a matter of fact, there is time interval of length π between these zeroes. Moreover, $\bar{s}^{-1}(z_1 \cos\alpha + z_2 \sin\alpha)$ is a periodic function of α. As a consequence, for every fixed $z_1 \in \Omega^z$ the scalar function $t(\tau, z)$ given by (38) is continuous and increasing function of τ with $t(\tau, z) \pm \infty$ as $\tau \to \pm\infty$. In other words, for every fixed $z_1 \in \Omega^z$ the relation (38) defines homeomorphism $\mathbb{R} \mapsto \mathbb{R}$. Since we already proved that z_1 is related to x_1 via the homeomorphism (30), the relations (38) and (30) give the homeomorphism $\mathbb{R} \times \Omega^x \mapsto \mathbb{R} \times \Omega^z$ requested by (22) in Definition 3.1. ■

To address the case of the perturbed damped HIPSF (7), consider its standard extension to an autonomous system by adding a formal state variable x_3 representing the time t, namely

$$
\begin{aligned}
\dot{x}_1 &= x_2,\\
\dot{x}_2 &= \frac{\theta_1 \sin x_1 - \theta_2 \mathrm{sign}(x_1) \cos x_1}{\theta}\\
&\quad - k_1 x_2 + \omega(x_3),\\
\dot{x}_3 &= 1, \quad k_1 \geq 0.
\end{aligned} \tag{39}
$$

Proposition 7. *Consider the perturbed damped HIPSF* (7) *and assume that there is some region* $\Omega^{xf} \subset \Omega^x$ *given by* (27) *such that* $\forall\, x_0 \in \Omega^{xf}$ *and* $\forall\, t_0 \in \mathbb{R}$, *the solution* $x(t, x_0)$ *of* (7) *exists and* $x(t, x_0) \in \Omega^{xf}\ \forall\, t \in \mathbb{R}$. *Moreover, assume that neither* $\lim_{t\to\infty} x(t, x_0) = 0$, *nor* $\lim_{t\to-\infty} x(t, x_0) = 0$. *Then the following system*

$$
\begin{aligned}
\frac{\mathrm{d}z_1}{\mathrm{d}\tau} &= z_2,\\
\frac{\mathrm{d}z_2}{\mathrm{d}\tau} &= -z_1 + \bar{s}(z_1)^{-1}(\omega(z_3) - k_1 z_2),\\
\frac{\mathrm{d}z_3}{\mathrm{d}\tau} &= \bar{s}(z_1)^{-1}, \quad z = (z_1, z_2, z_3)^\top \in \Omega^{zf} \times \mathbb{R},
\end{aligned} \tag{40}
$$

is topologically equivalent to (39) *given* $\Omega^{xf} \times \mathbb{R}$. *Here* Ω^{zf} *is the image of* Ω^{xf} *via the homeomorphism* (30) *and* $\bar{s}(z_1)$ *is given by* (36).

Proof. To prove the proposition claim, it has to be shown first that the homeomorphism (30) and $z_3 = x_3$ together with the time scaling $\bar{s}(z_1)$ given by (36) transform (39) into (40). Then, secondly, it has to be shown that the time scaling $\bar{s}(z_1)$ given by (36) actually defines the time transformation $t \to \tau$ required in Definition 3.1. The first part is straightforward. Realizing that $z_3(\tau) = t\ \forall\, t \in \mathbb{R}$, it basically mimics the proof of Proposition 6. To prove the second part, note first that it is not obvious that $\int_0^\tau \bar{s}(z_1(\alpha))^{-1}\mathrm{d}\alpha \to \pm\infty$ for $t \to \pm\infty$. Indeed, since there is no closed form of solution $z_1(\tau)$, no simple analysis of its zero values as in the proof of Proposition 6 is possible. Nevertheless, one can prove that $\int_0^\tau \bar{s}(z_1(\alpha))^{-1}\mathrm{d}\alpha \to \pm\infty$ for $t \to \pm\infty$ using the famous Barbalat lemma and properties of the autonomous extension (39). Indeed, the right-hand side of (40) is globally Lipschitz and therefore $z(\tau)$ exists and is unique for any given initial condition and by (36) the integral $\int_0^\tau \bar{s}(z_1(\alpha))^{-1}\mathrm{d}\alpha$ is a nondecreasing function defined as $\forall\, \tau \in \mathbb{R}$. If the function $\int_0^\tau \bar{s}(z_1(\alpha))^{-1}\mathrm{d}\alpha$ is bounded from above (below), it converges as $\tau \to \infty$ ($\tau \to -\infty$) to some constant positive (negative) finite value x_3^{fp} (x_3^{fm}). Further, $z_1(\tau)$ is obviously uniformly continuous on $\mathbb{R}$ due to the first equation in (40). Therefore also $\bar{s}(z_1(\tau))^{-1}$ is uniformly continuous on $\mathbb{R}$ and therefore by Barbalat lemma $z_3(\tau) \to z_3^{fp} \in \mathbb{R}$, $\tau \to \infty$ ($z_3(\tau) \to z_3^{fm} \in \mathbb{R}$, $\tau \to -\infty$) implies that $\bar{s}(z_1(\tau))^{-1} \to 0$, $\tau \to \pm\infty$, therefore also $z_1(\tau) \to 0$, $\tau \to \pm\infty$. This means that the ω-limit set (the α-limit set) of (40) is the Cartesian product of $\{z_3^{fp}\}$ ($\{z_3^{fm}\}$) and the ω-limit set (the α-limit set) of

$$
\frac{\mathrm{d}z_1}{\mathrm{d}\tau} = z_2, \quad \frac{\mathrm{d}z_2}{\mathrm{d}\tau} = 0,
$$

which is the origin since, due to the time invariance of the system, ω-limit set (α-limit set) should be invariant. Therefore, $x(t) \to 0$, $t \to x_3^f$, due to the homeomorphic correspondence of the trajectories of the HIPSF (7) and (40). Summarizing, unless the perturbed and damped HIPSF (7) is asymptotically stable at some nonzero initial condition, or unbounded, it is always topologically equivalent to (40) on the regions specified by the proposition assumption. ■

Remark 3.1. Proposition 7 and the equivalent system (40) help to understand the behavior of the perturbed undamped HIPSF. First, realize that $\bar{s}(z_1)^{-1} \geq 0$ given by (36) is smooth except $z_1 = 0$, where it is Lipschitz and therefore the equivalent system (40) is also similar. Further, recall that $z_3(\tau) = t$, so that z_1, z_2 in (40) behave the same way as in the following system

$$\frac{\mathrm{d}z_1}{\mathrm{d}\tau} = z_2, \quad \frac{\mathrm{d}z_2}{\mathrm{d}\tau} = -z_1 + \bar{s}(z_1)^{-1}(\omega(t) - k_1 z_2),$$
$$z = (z_1, z_2)^\top \in \Omega^{zf}. \quad (41)$$

Let us consider for simplicity the case $k_1 = 0$ since the damping is anyway usually rather weak and does not have a significant effect. Then the system (41) is the linear oscillator in the "new" scaled time τ perturbed by a signal $\omega(t)$ being harmonic in the "real" time t. Moreover, its amplitude is multiplied by the nonlinear function $\bar{s}(z_1)^{-1}$. Close to $z_1 = 0$, both τ is slowing down with respect to t ($\bar{s}(z_1)^{-1}$ is the scaling between τ and t) and the amplitude is made smaller as it is multiplied by $\bar{s}(z_1)^{-1}$. Far from $z_1 = 0$ such an effect is weak. Notice, that

$$\frac{\mathrm{d}}{\mathrm{d}\tau}(z_1^2 + z_2^2) = \bar{s}(z_1)^{-1}\omega(t)z_2^2 - k_1\bar{s}(z_1)^{-1}z_2^2,$$
$$k_1 \geq 0, \ \ \bar{s}(z_1)^{-1} \geq 0,$$

therefore (when $k_1 = 0$) the norm of $(z_1, z_2)^\top$ increases when $\omega(t) > 0$ and decreases when $\omega(t) < 0$. Due to the above complex effect of change of time and amplitude, neither of these two conditions holds prevailing time. Therefore the norm alternates between increasing and decreasing, moreover, the norm increase leads to a prevalently bigger absolute value of $\bar{s}(z_1)^{-1} \geq 0$, while the norm decrease leads to a prevalently smaller absolute value of $\bar{s}(z_1)^{-1} \geq 0$. Such a complex effect may serve as an explanation of the irregular chaotic behavior observed and justified numerically later on.

Remark 3.2. Consider the unforced HIPSF (7). One of the consequences of the time scaling by $\bar{s}(z_1)^{-1} \geq 0$, demonstrated numerically later on, is that in the original "real" time t the oscillations of the HIPSF have the period converging to zero when their initial conditions converge to the origin. Indeed, in the unforced case the HIPSF oscillations are simply obtained as the superposition of the harmonic oscillations in the "new" time τ and the time scaling transformation between the "new" time τ and the "real" time t. The effect of that scaling transformation is stronger for the oscillations closer to the origin than for those farther from the origin. In such a way, the unforced HIPSF self-oscillations frequencies are growing to infinity as their magnitude goes to zero which is intuitively clear from the mechanical viewpoint as well. Such a property is somehow exceptional (cf. Example 3.1 later on), it is due to the hybrid essence of the HIPSF. At the same time, such a period goes to infinity, when trajectories approach the separatrices — boundaries of the region of the stable behavior of the unperturbed undamped HIPSF. These phenomena are demonstrated by the closed orbits shown in Fig. 4 and computed HIPSF frequencies of the periodic motions on those closed curves are collected in Table 1. This gives the following interesting clue to study the influence of the harmonic perturbation: it may be in the "bad", i.e. the destabilizing, phase synchronization for some fixed amplitude only, increasing the amplitude by destabilization changes the hybrid pendulum frequency and the stabilizing effect may occur. In such a way, the bounded chaotic behavior may be intuitively explained. Moreover, as HIPSF frequencies go to infinity as their magnitude goes to zero, the chaotic behavior of the perturbed undamped HIPSF can be observed later on arbitrarily close to the origin.

Example 3.1. Consider the well-known nonlinear pendulum oscillating around its lower stable position and not reaching its upward (inverted) position, i.e.

$$\dot{x}_1 = x_2, \quad \dot{x}_2 = -\sin(x_1), \quad x_1 \in (-\pi, \pi), \ \ x_2 \in \mathbb{R}.$$

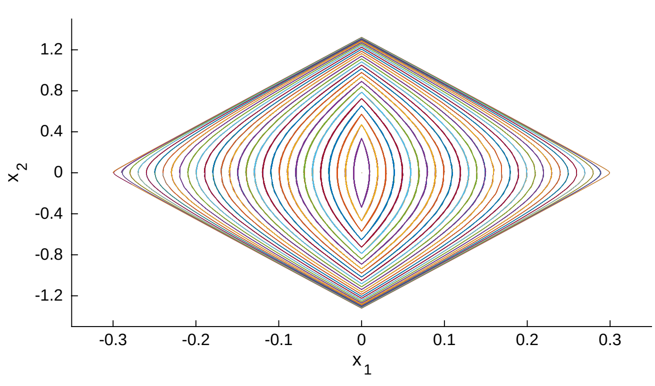

Fig. 4. Orbits of the undamped unperturbed ($k_1 = 0$, $\omega(t) \equiv 0$) HIPSF (7) for $\theta_1 = 3.4433, \theta_2 = 1.0791, \theta = 0.1891$.

Table 1. Dependence of the undamped unperturbed ($k_1 = 0$, $\omega(t) \equiv 0$) HIPSF oscillations frequency fr on their initial condition $(x_1, 0)^\top$ for $\theta_1 = 3.4433, \theta_2 = 1.0791, \theta = 0.1891$.

x_1 [rad]	0.3	0.25	0.2	0.15	0.1	0.05	0.01	10^{-3}	10^{-4}	10^{-5}	10^{-6}	10^{-7}	10^{-8}	10^{-9}
fr [Hz]	0.25	0.47	0.69	0.92	1.25	1.93	3.49	14.64	46.4	146.5	463.6	1466	4636	14 663

Introduce new coordinates $z = (z_1, z_2)^\top$ and time $\tau(t, x)$ as follows

$$z_1 = 2\sin\left(\frac{x_1}{2}\right), \quad z_2 = x_2, \quad \frac{\mathrm{d}\tau}{\mathrm{d}t} = \cos\left(\frac{x_1}{2}\right).$$

Inverse transformations are

$$x_1 = 2\arcsin\left(\frac{z_1}{2}\right), \quad x_2 = z_2, \quad \frac{\mathrm{d}t}{\mathrm{d}\tau} = \frac{\sqrt{4 - z_1^2}}{2}.$$

Straightforward computations show that the nonlinear pendulum takes in z-coordinates of the following form

$$\frac{\mathrm{d}z_1}{\mathrm{d}\tau} = z_2, \quad \frac{\mathrm{d}z_2}{\mathrm{d}\tau} = -z_1, \quad z_1 \in (-2, 2), \ \ z_2 \in \mathbb{R},$$

which is the linear harmonic oscillator. Unlike the HIPSF case considered above, all the above transformations are smooth and smoothly invertible on the above regions with time scaling being smooth, nonzero and finite as well. Moreover, time scaling is equal to 1 at the origin and the coordinate change is approximately equal to identity map in a small neighborhood of the origin. The latter property reflects the fact that the approximate linearization of the nonlinear pendulum is precisely the same linear harmonic oscillator given above. As a consequence, the periodic movements of the undamped nonlinear pendulum have the lower limit of their periods equal to 2π which is the period of that linear harmonic oscillator. Contrary to that, the scaling $s(x)$ for the HIPSF case ranges from zero to infinity and it is only continuous and continuously invertible. As a consequence, the unforced HIPSF exhibits oscillations with periods ranging from zero to infinity. These phenomena are demonstrated by the closed orbits shown in Fig. 4 and the computed HIPSF frequencies on those closed curves collated in Table 1.

4. Numerical Simulations

4.1. *On the calculation of the largest Lyapunov exponent*

To test the possible chaotic behavior numerically, the largest Lyapunov exponent will be computed. The purpose of this very short subsection is to present the method for these computations used later on.

As noticed in [Licskó & Csernák, 2014], calculating the Lyapunov spectrum or even only the largest Lyapunov exponent (LLE) can be difficult in case of piecewise-smooth systems. Methods usually used for smooth systems often fail because of discontinuities. One of the possible methods for the estimation of the LLE is based on the calculation of the coupling coefficient that imposes synchronization between two coupled systems [Stefański, 2000; Stefański & Kapitaniak, 2003]. The smallest value of the coupling coefficient for which the synchronization takes place is claimed to be equal to the LLE, see [Stefański & Kapitaniak, 2000] where the LLE for Duffing oscillator with dry friction was calculated. This method was also implemented to estimate the LLE in the multibody system in [Fu & Wang, 2006].

More specifically, following Stefański [2000], consider two coupled perturbed undamped HIPSF:

$$\begin{aligned}
\dot{x}_1 &= x_2, \\
\dot{x}_2 &= \frac{\theta_1 \sin x_1 - \theta_2 \mathrm{sign}(x_1)\cos x_1}{\theta} + \omega(t), \\
\dot{y}_1 &= y_2 + c(x_1 - y_1), \\
\dot{y}_2 &= \frac{\theta_1 \sin y_1 - \theta_2 \mathrm{sign}(y_1)\cos y_1}{\theta} \\
&\quad\quad + \omega(t) + c(x_2 - y_2).
\end{aligned} \tag{42}$$

Local synchronization of the coupled systems (42) is therefore achieved if (and only if) the coupling gain c is larger than the LLE, [Baumann & Leine, 2017]. In other words, the infimum of the values of the coupling coefficient c for which synchronization takes place is equal to the LLE, [Stefański & Kapitaniak, 2000]. The coupled system is considered to be synchronized if the synchronization error $e = x - y$ becomes smaller than a certain threshold on a long but finite time horizon.

The practical problem here is the precise determination of the LLE. Indeed, the LLE is the infimum of values of c providing the above synchronization. It is clear, that for the values of c close to that infimum, the synchronization is obtained only after a long time course. Alternatively, the desynchronization detection for the values of c less than the corresponding LLE can be used adapting the desynchronization detection approach in [Lynnyk & Čelikovský, 2010; Čelikovský & Lynnyk, 2012]. Moreover, to provide some ground for the claim, that the studied behavior is chaotic, it is sufficient just to show that the above coupling parameter is positive and the precise value of the respective LLE is not needed. The subsequent simulations are therefore usually limited to showing that there is some positive c ensuring synchronization and some smaller, yet still positive c, such that the master-slave configuration (42) remains desynchronized.

Another numerical issue is related to the phenomena at the discontinuity. As a consequence, in some simulations close to the origin where the discontinuity is crossed very frequently, computational difficulties do not allow the precise determination of the LLE. The respective LLE estimations are skipped as they were rather misleading.

4.2. *Simulations of the harmonically perturbed HIPSF*

The influence of the external harmonic perturbing signal $\omega(t)$ will be systematically studied here. Remind, that (15) indicates that the external perturbation influence is hard to be estimated theoretically. Obviously, when $x_2(t)\omega(t) > 0$, that influence is destabilizing, when $x_2(t)\omega(t) < 0$, it is stabilizing. As a matter of fact, the hybrid inverted pendulum is strictly passive for $k_1 > 0$ and it is passive for $k_1 = 0$. In all these passivity cases the input is ω, the output is x_2 and the storage function is V as given by (14). As the frequencies of HIPSF natural oscillations vary from zero to infinity depending on their magnitudes, external harmonic perturbation preserves neither the relation $x_2(t)\omega(t) > 0$, nor the relation $x_2(t)\omega(t) < 0$ all the time. Such an effect results in the magnitude variation in an irregular way. Using LLE estimation, the chaotic character of that irregularity will be argued.

The following parameters are used in all subsequent simulations: $I_L = I_R = 0.0062$, $I_D = 0.00066$, $I_T = 0.0158$, $d = 0.2$, $m = 0.4$, $l_L = l_R = 0.22$, $l = 0.5$, $l_T = 0.1$, $M_T = 0.25$, $M_D = 0.05$, $g = 9.81$, given in $\text{kg}\cdot\text{m}^2$, m, kg, $\text{m}\cdot\text{s}^{-2}$, respectively. These parameters give $\theta_1 = 3.4433$, $\theta_2 = 1.0791$, $\theta = 0.1891$ in (7). For the simplicity, only the case of the undamped ($k_1 = 0$) HIPSF (7) is considered.

To demonstrate the time evolution more visibly, all simulations are split into ten subsequent equally long time subintervals. The blue, red and green colors are then regularly switched for the trajectory drawing line between these intervals. This applies to the planar state space plots where the time course cannot be indicated explicitly. Other plots of some scalar values against the time are kept monochromatic. Note the interesting property in some state space trajectory simulations plots close to the origin. They appear to be monochromatic, but that is due to the fact that the trajectory evolution is getting faster and faster as time goes on. As a consequence, the last time segment trajectory is much longer than the previous ones and it overwrites them.

The sizes and shapes of the possibly chaotic attractors depend on the perturbation frequency, the perturbation amplitude and the initial conditions $x_1(0)$, $x_2(0)$. To sort these three aspects in some reasonable synoptical way, let us first split simulations into two basic groups dependent on the perturbation amplitude and its relation to the stability threshold $A = \theta_2/\theta = 5.7065$ introduced in Proposition 2 and explained by Remark 2.4. Recall, that the undamped HIPSF perturbed by a constant external perturbation having absolute value less than the threshold $A = \theta_2/\theta$ has the trivial solution starting at the origin, moreover, this solution is unique and asymptotically stable. For the nonconstant external harmonic perturbation, even having the amplitude less than the threshold $A = \theta_2/\theta$, such a property cannot be guaranteed. Nevertheless, the HIPSF behavior, when affected by the external harmonic forcing, is qualitatively different for the amplitudes less than the threshold $A = \theta_2/\theta$ and for those greater than it.

To proceed with the above plan, let us start first with the case when the amplitude of the perturbation signal is fixed and bigger than the threshold $A = 7 > \theta_2/\theta = 5.7065$. Figure 5 shows the complex behavior of the HIPSF for the different values of the frequency of the bounded external perturbation $\omega(t)$, while the initial conditions are fixed and very close to the origin, i.e. $x_1 = 10^{-12}$ and $x_2 = 0$. Yet, they result in a growing trajectory appearing chaotically. There is a clearly visible relation between the attractor size and forcing

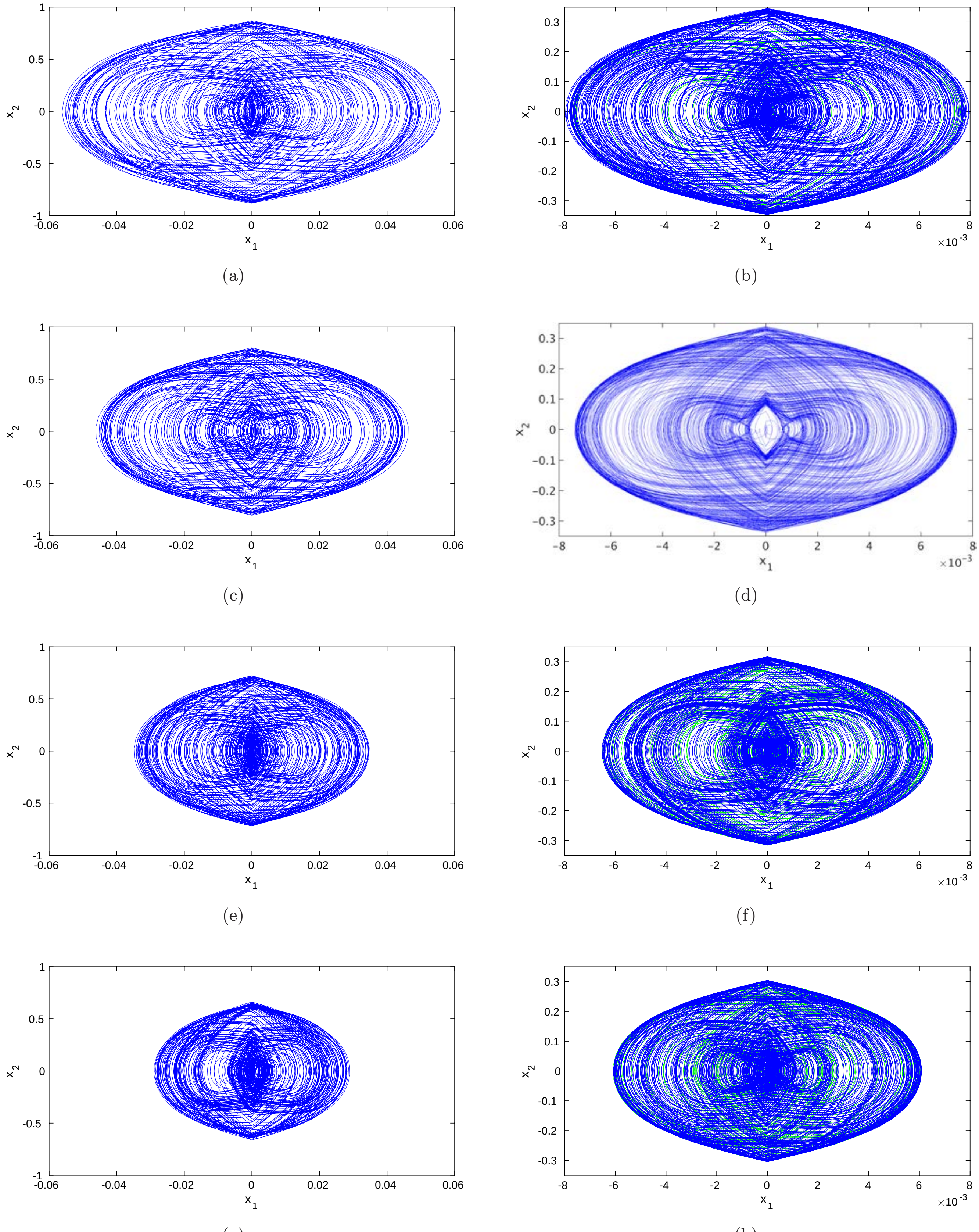

Fig. 5. Complex behavior of (7) for $x_1(0) = 10^{-12}, x_2(0) = 0, k_1 = 0, t \in [0, 50]$. External forcing signals $\omega(t)$ are: (a) $7\sin 8\pi t$; (b) $7\sin 21\pi t$; (c) $7\sin 9\pi t$; (d) $7\sin 22\pi t$; (e) $7\sin 10\pi t$; (f) $7\sin 23\pi t$; (g) $7\sin 11\pi t$ and (h) $7\sin 24\pi t$.

frequency, namely, a higher frequency results in a smaller size of the attractor, and a lower frequency in a bigger size of the attractor. Explanation is that the attractor size is related to the frequency of the HIPSF, which should be along that trajectory slightly bigger or slightly smaller than the forcing one. Recall in this respect, Table 1 showing the relation between the own unperturbed undamped HIPSF oscillations frequency and the magnitude of these oscillations. Note, that the case in Fig. 5(a) (the smallest frequency and the highest attractor size) appears to be bounded, but that is only due to the limited time course duration $t \in [0, 50]$. On the longer time interval $[0, 232]$ the oscillations exceed the region bounded by separatrices, as shown in Fig. 6(a). Physically such a situation corresponds to the HIP falling to the other side of one of the unstable classical saddle point equilibria. Interestingly, increasing the size of initial condition keeping the same frequency as in Figs. 5(a) and 6(a)

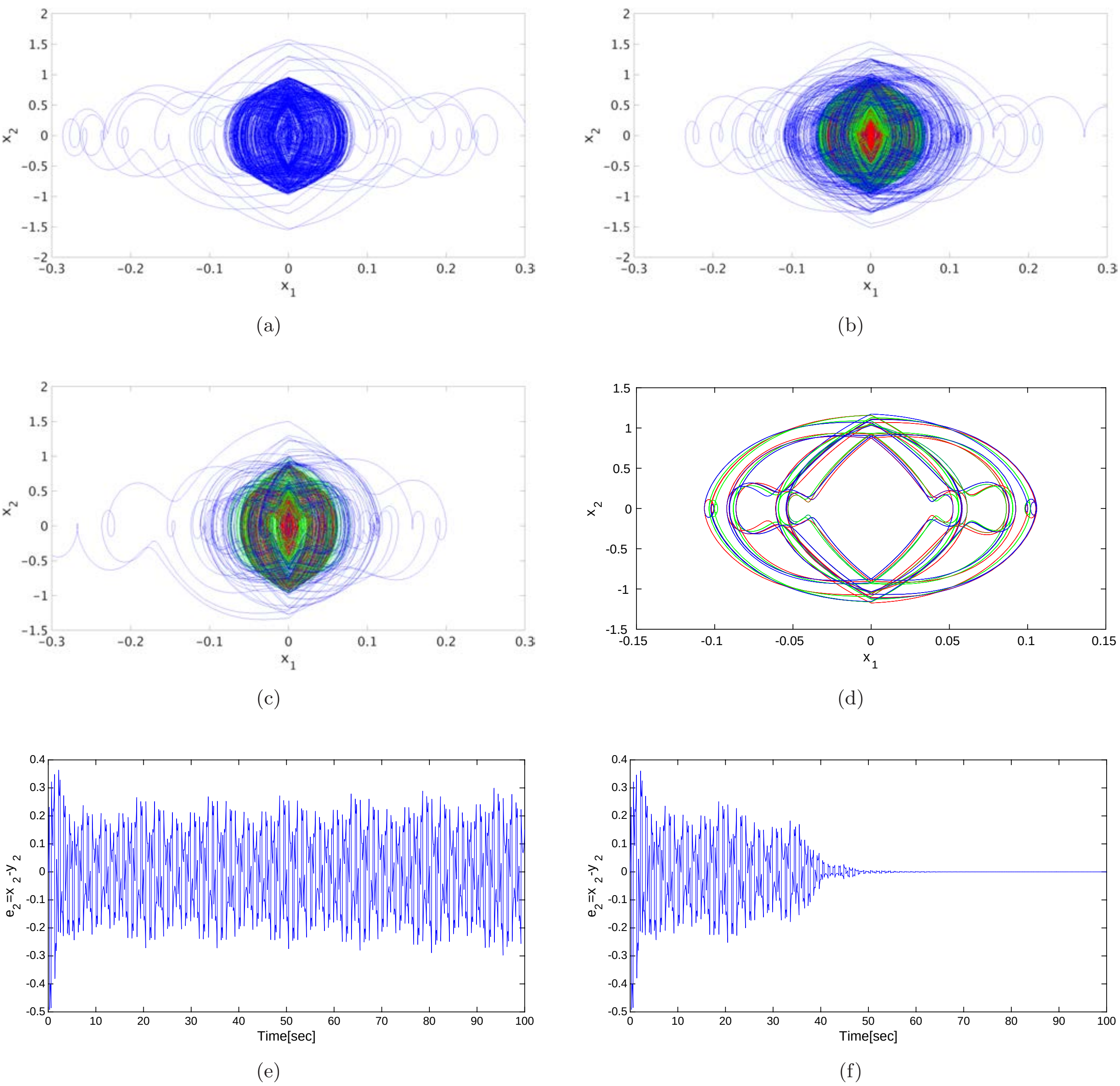

(a) (b) (c) (d) (e) (f)

Fig. 6. State space plots of (7): $x_2(0) = 0$, $k_1 = 0$, $\omega(t) = 7\sin 8\pi t$ and: (a) $x_1(0) = 10^{-12}$, $t \in [0, 232]$; (b) $x_1(0) = 10^{-6}$, $t \in [0, 883]$; (c) $x_1(0) = 10^{-3}$, $t \in [0, 358]$; (d) $x_1(0) = 10^{-1}$, $t \in [0, 50]$; (e) and (f) illustrate LLE $\in (0.215, 0.22)$ for (d).

does not have a straightforward effect. First, the escape time gets shorter, cf. Figs. 6(b) and 6(c), but then for much bigger initial condition, the attractor stays inside the required region even during a very long time interval, see Fig. 6(d). For space reasons, the time duration is limited there to the interval $[0, 50]$ only, but the trajectory stays inside the stable region during the duration of every experiment that was reasonably long to be carried out. The chaotic essence of the case in Fig. 6(d) is supported by the LLE estimate in Figs. 6(e) and 6(f), indicating that the LLE should be within $(0.215, 0.22)$. As already indicated before, computations of the LLE for the cases of small attractors close to the origin failed due to the previously mentioned numerical issues caused by the frequent crossing of the discontinuity at $x_1 = 0$.

Secondly, let us present the case when the amplitude of the external harmonic perturbation is less than the threshold $\theta_2/\theta = 5.7065$. In this

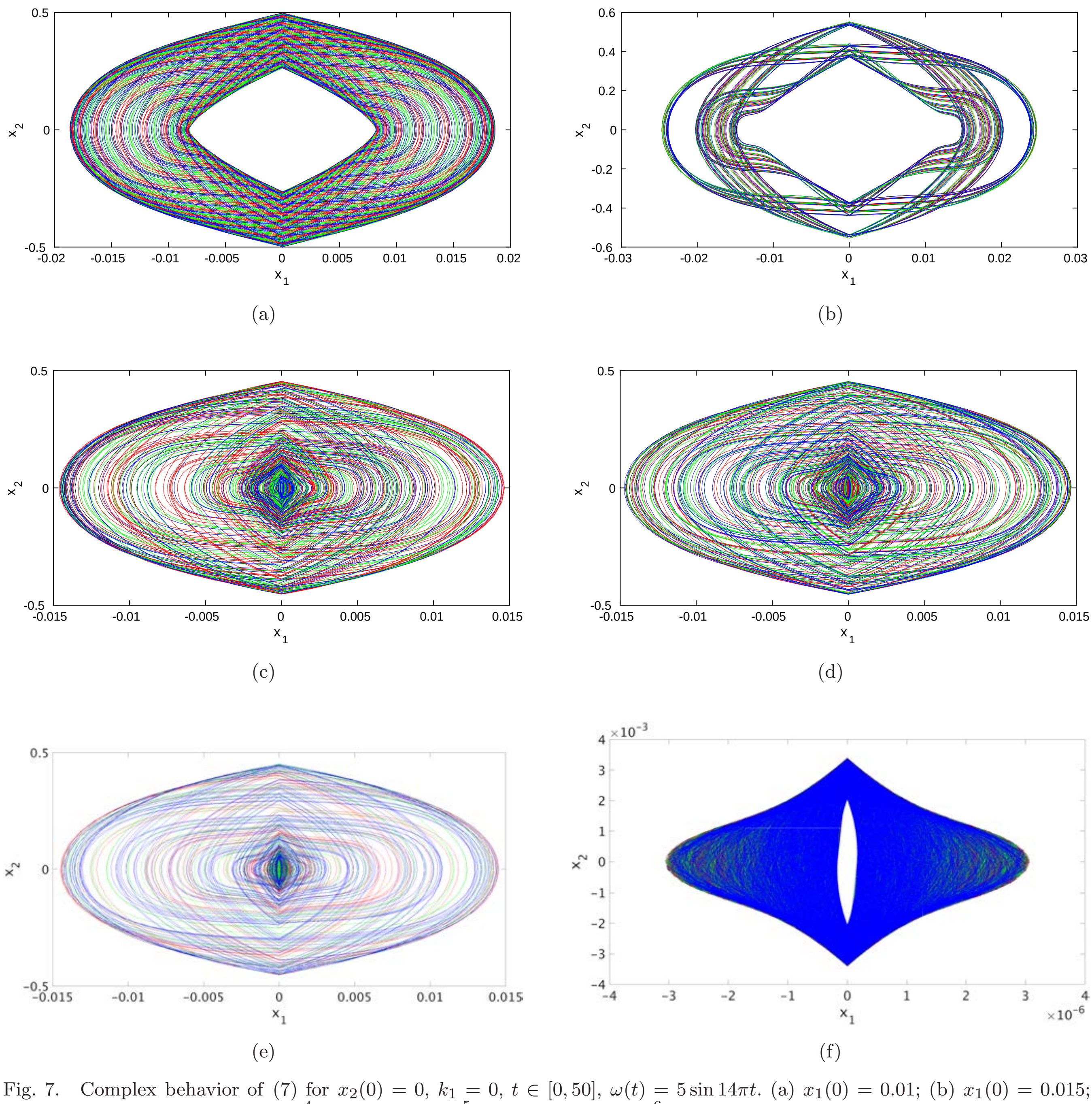

Fig. 7. Complex behavior of (7) for $x_2(0) = 0$, $k_1 = 0$, $t \in [0, 50]$, $\omega(t) = 5 \sin 14\pi t$. (a) $x_1(0) = 0.01$; (b) $x_1(0) = 0.015$; (c) $x_1(0) = 0.005$; (d) $x_1(0) = 10^{-4}$; (e) $x_1(0) = 10^{-5}$ and (f) $x_1(0) = 10^{-6}$.

case, the trajectory stays very close to the initial condition for the initial condition $x_1(0) = 10^{-6}$, $x_2(0) = 0$, see Fig. 7(f). Nevertheless, when the initial conditions are $x_1 \geq 10^{-5}$ then the chaotically appearing attractors emerge and their size, though rather small, is by several orders bigger than the respective initial condition, see Fig. 7 showing different attractors for different initial conditions

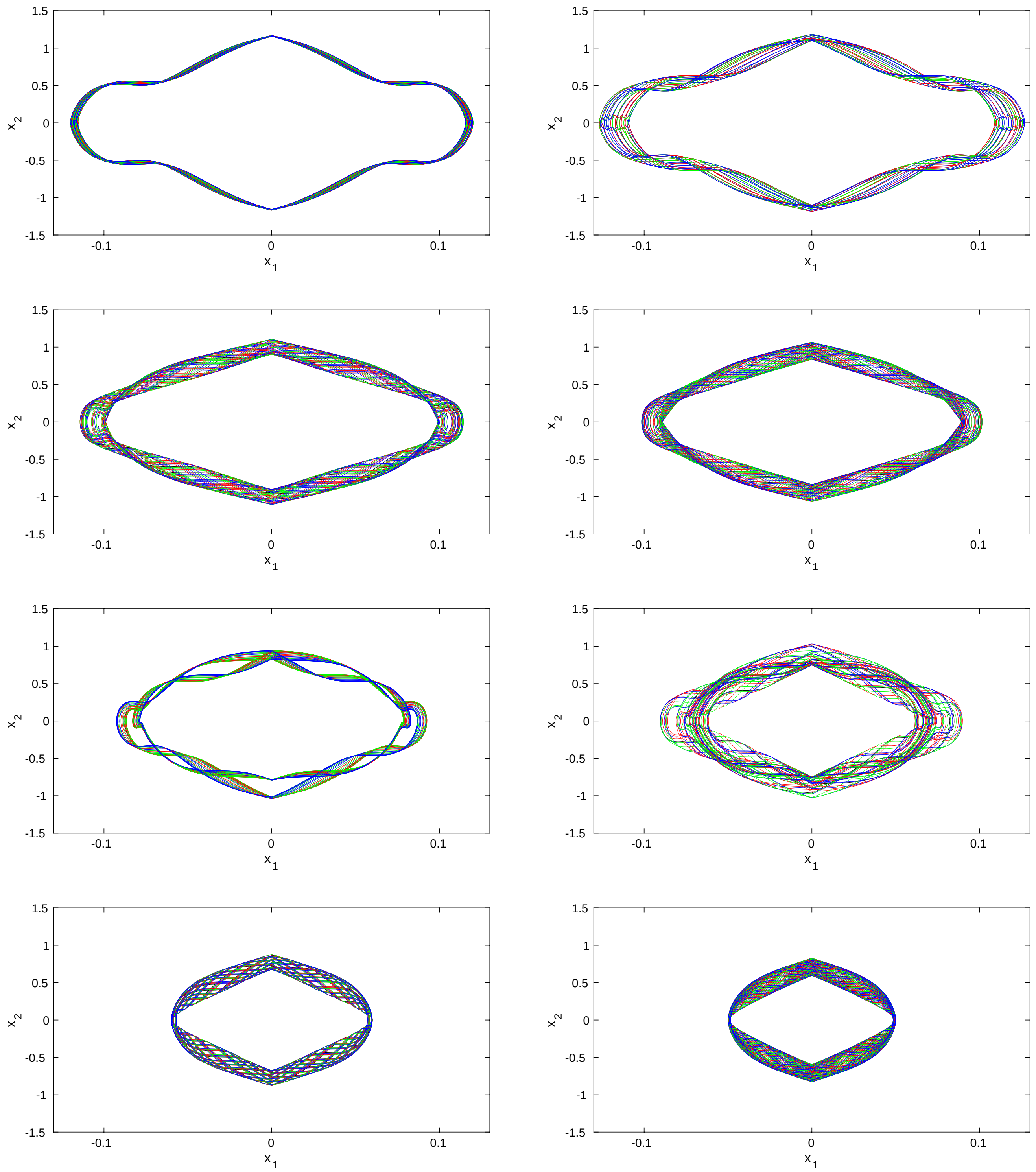

Fig. 8. Multiple hidden attractors in (7) for $x_2(0) = 0$, $k_1 = 0$, $t \in [0, 50]$, $\omega(t) = 5 \sin 14\pi t$ and various $x_1(0)$. Row-by-row, from the left to the right: $x_1(0) = 0.12$; $x_1(0) = 0.11$; $x_1(0) = 0.1$; $x_1(0) = 0.09$; $x_1(0) = 0.08$; $x_1(0) = 0.07$; $x_1(0) = 0.06$; $x_1(0) = 0.05$.

$x_1(0)$. Note, that the attractors shown in Fig. 7 may overlap each other, this is not a contradiction, recall that the simulated dynamics is nonautonomous. Further, increasing the initial conditions even more, different chaotically appearing attractors emerge and this time all of them are clearly disjoint, see Fig. 8. This is a very interesting phenomenon. Realize, that all simulations in Figs. 7

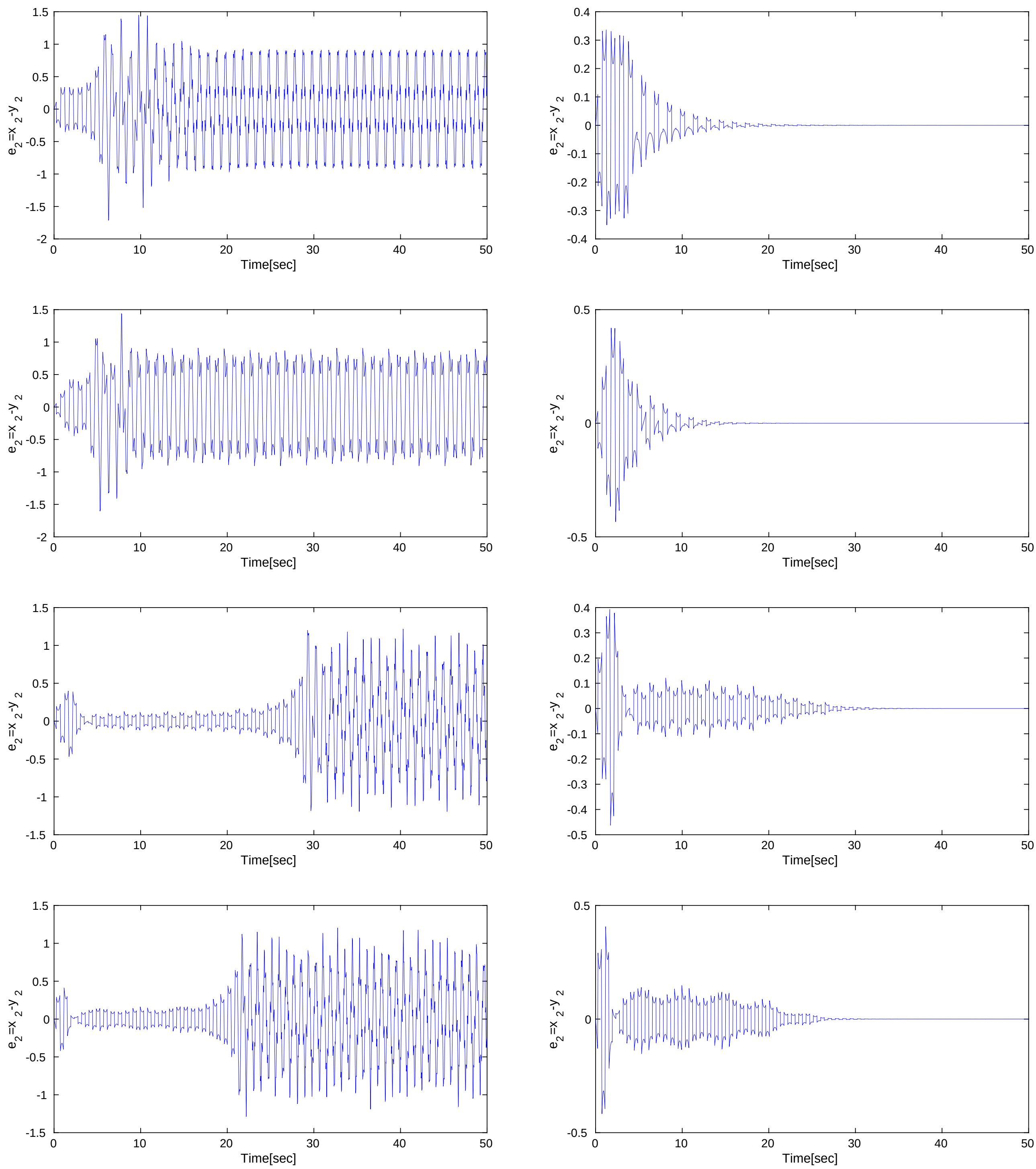

Fig. 9. The synchronization error $e_2 = x_2 - y_2$ for the coupled HIPSFs corresponding to the cases shown in Fig. 8. From the top to the bottom, the cases from the top left to the bottom right in Fig. 8 are shown. The left (right) column shows the synchronization error divergence (convergence) for the lower (upper) LLE estimate. The respective ranges of LLE are: $[0.253, 0.254]$; $[0.33, 0.333]$; $[0.56, 0.57]$; $[0.79, 0.8]$; $[0.91, 0.92]$; $[0.7, 0.71]$; $[0.36, 0.37]$; $[0.52, 0.527]$.

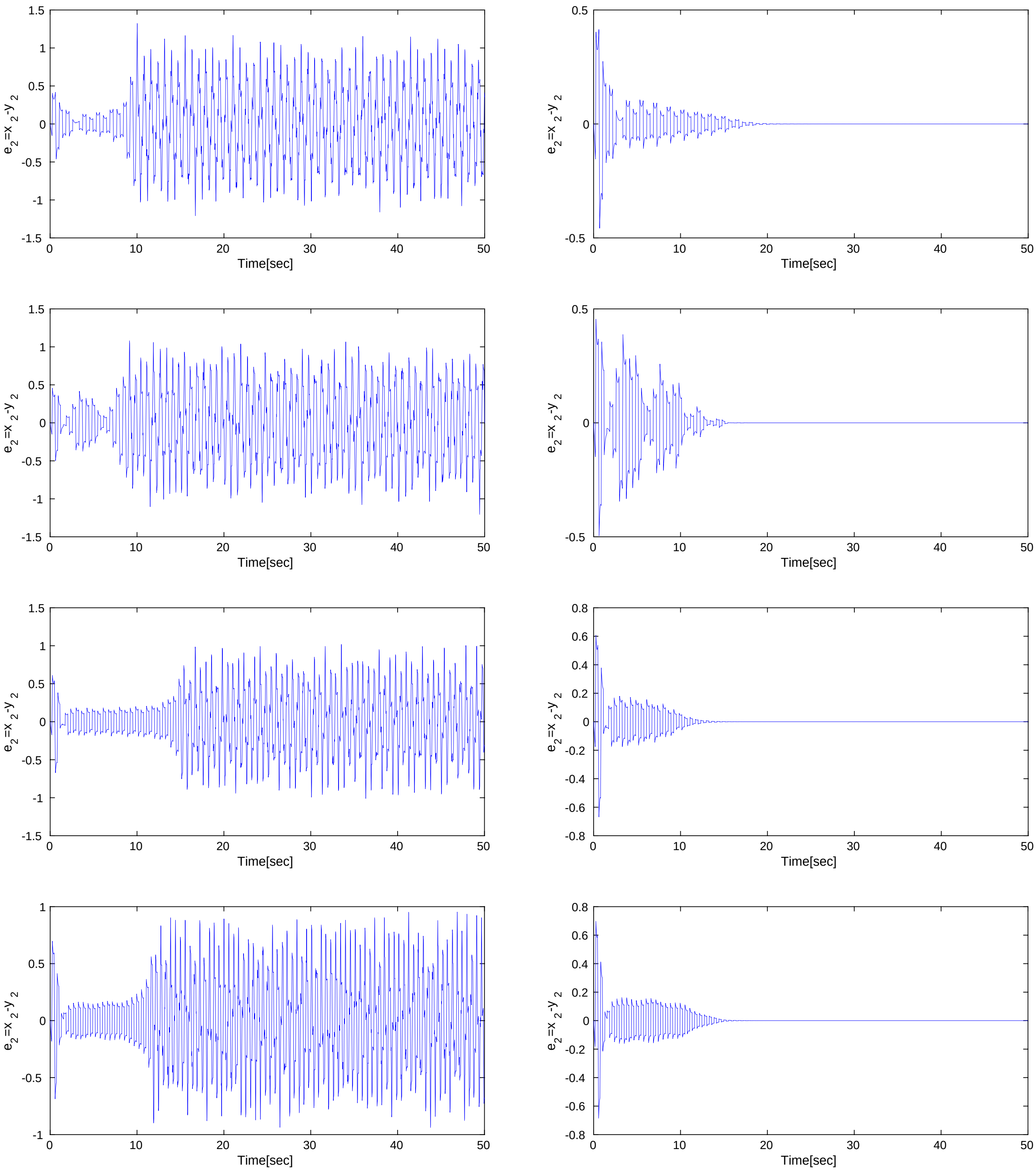

Fig. 9. (*Continued*)

and 8 show the same system with the same forcing, only initial conditions are different. Moreover, as already noted, all attractors shown in Fig. 8 are clearly disjoint. In such a way, it is possible to claim that the so-called **multiple hidden attractors** in the sense of Leonov–Kuznetsov [Leonov *et al.*, 2011; Leonov & Kuznetsov, 2013; Chen *et al.*, 2017] are present in the respective HIPSF. This means that several attractors are present in the system, all of them have different basins of attraction and not one of these basins of attraction contains the origin. Our conjecture here is that there may be even

infinite number of these attractors, unfortunately, one cannot demonstrate such a conjecture experimentally. Intuitive explanation of the existence of multiple hidden attractors is that each of these attractors correspond to an individual multiple of the perturbation frequency that fits to some suitable HIPSF frequency. Remember that the unperturbed HIPSF frequency goes to zero as HIPSF oscillations approach the separatrices and therefore theoretically infinite number of multiples of those frequencies is possible. Practically, nevertheless, all these behaviors should be placed within increasingly narrow area close to separatrices. In such a way, another peculiarity when trying to simulate more attractors close to separatrices is that they can easily escape the "safe" region inside the separatrices during the transition process.

To support the claim that the attractors shown in Fig. 8 are chaotic, Fig. 9 shows the appropriate values of the LLEs for all attractors from Fig. 8. Note, that all these LLEs are clearly positive, i.e. there is sufficiently large gap between zero and those lower LLE estimates. As already noted, for the attractors shown in Fig. 7, numerical issues related to frequent crossing of the right-hand side discontinuity prevented obtaining reasonable LLE estimates and the corresponding simulations are skipped.

Finally, Fig. 10 demonstrates yet another HIPSF with multiple hidden attractors, namely, for

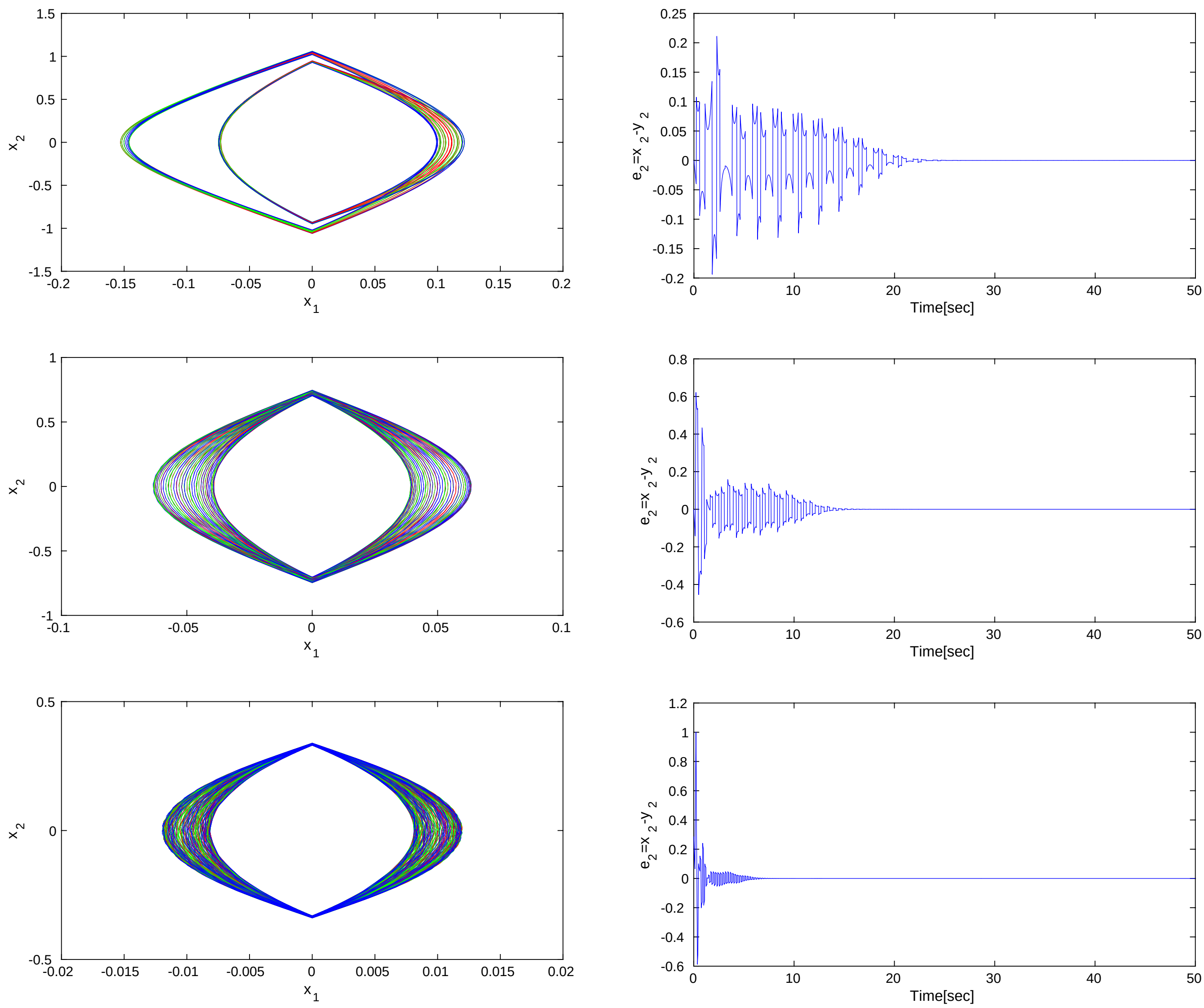

Fig. 10. Complex behavior of (7) for $x_2(0) = 0$, $k_1 = 0$, $\omega(t) = \sin \pi t$, $t \in [0, 50]$ and various initial values $x_1(0)$. The left side shows the state trajectories while the right side shows $e_2 = x_2 - y_2$ for the practically smallest coupling parameter c providing the synchronization. From the top to the bottom: $x_1(0) = 0.1$, $c = 0.91$; $x_1(0) = 0.05$, $c = 1.31$; $x_1(0) = 0.01$, $c = 2.3$.

the forcing external signal $\sin \pi t$. Again, the size of the attractor depends on the initial conditions $x(0)$, attractors appear to be mutually disjoint and their basins of attraction do not contain the origin. The estimates of the corresponding LLEs are included in the same figure, for brevity, only the courses of the synchronizing coupling parameters are included. In all cases, even a negligible decrease of the coupling parameter leads to synchronization failure. The values noted in the caption of Fig. 10 are therefore quite fair estimates of the appropriate LLEs.

5. Conclusions

The properties of the harmonically perturbed hybrid inverted pendulum have been studied. An interesting feature is the presence of the multiple hidden chaotic attractors when the perturbing amplitude does not exceed the well-defined threshold. Namely, basins of attraction of these attractors do not contain the origin and are mutually disjoint. Detailed proofs of the existence, stability and other basic mathematical properties, including topological linearizability of the hybrid inverted pendulum in the state space form were provided as well. A challenging outlook for future research is to use topological linearization for the better computation of the minimal coupling coefficient in the simple master-slave configuration to determine the largest Lyapunov exponent. Indeed, even the perturbed damped hybrid inverted pendulum in the state space form is topologically equivalent to a system with the Lipschitz right-hand side where the numerical issues caused by the discontinuity are avoided.

References

Baumann, M. & Leine, R. I. [2017] "Synchronization-based estimation of the maximal Lyapunov exponent of nonsmooth systems," (*24th Int. Congr. Theoretical and Applied Mechanics*) *Procedia IUTAM* **20**, 26–33.

Butikov, E. I. [2008] "Extraordinary oscillations of an ordinary forced pendulum," *Eur. J. Phys.* **29**, 215–233.

Čelikovský, S. & Lynnyk, V. [2012] "Desynchronization chaos shift keying method based on the error second derivative and its security analysis," *Int. J. Bifurcation and Chaos* **22**, 1250231-1–11.

Čelikovský, S. & Anderle, M. [2016] "Hybrid invariance of the collocated virtual holonomic constraints and its application in underactuated walking," *Preprints of the 10th IFAC Symp. Nonlinear Control Systems* (Monterey, California, USA), pp. 802–807.

Čelikovský, S. & Anderle, M. [2017] "Collocated virtual holonomic constraints in Hamiltonian formalism and their application in the underactuated walking," *Proc. 11th Asian Control Conf.* (*ASCC*) (Gold Coast, Australia), pp. 192–197.

Čelikovský, S. & Lynnyk, V. [2018a] "On the chaotic dynamics in the hybrid inverted pendulum," *Proc. 5th IFAC Conf. Analysis and Control of Chaotic Systems* (*CHAOS 2018*) (Eindhoven, Netherlands), pp. 21–27.

Čelikovský, S. & Lynnyk, V. [2018b] "On the hybrid inverted pendulum dynamics and its relation to the lateral stability of the walking-like mechanical systems," *Proc. Second IFAC Conf. Modelling, Identification and Control of Nonlinear Systems* (*MICNON*) (Guadalajara, Mexico), pp. 496–501.

Chen, G., Kuznetsov, N. V., Leonov, G. A. & Mokaev, T. N. [2017] "Hidden attractors on one path: Glukhovsky–Dolzhansky, Lorenz, and Rabinovich systems," *Int. J. Bifurcation and Chaos* **27**, 1750115-1–9.

Chevallereau, C., Abba, G., Aoustin, Y., Plestan, F., Westervelt, E. R., Canudas-De-Wit, C. & Grizzle, J. W. [2003] "Rabbit: A testbed for advanced control theory," *IEEE Contr. Syst.* **23**, 57–79.

Chevallereau, C., Bessonnet, G., Abba, G. & Aoustin, Y. [2009] *Bipedal Robots*: *Modeling, Design and Walking Synthesis* (Wiley-ISTE).

Dolinský, K. & Čelikovský, S. [2012] "Adaptive nonlinear tracking for robotic walking," *Cybernet. Phys.* **1**, 28–35.

Dolinský, K. & Čelikovský, S. [2018] "Application of the method of maximum likelihood to identification of bipedal walking robots," *IEEE Trans. Contr. Syst. Technol.* **26**, 1500–1507.

Dua, A. & Marathe, A. [2015] "Computing Melnikov curves for periodically perturbed piecewise smooth oscillators," *Int. J. Bifurcation and Chaos* **25**, 1550067-1–18.

Filippov, A. F. [1988] *Differential Equations with Discontinuous Righthand Sides* (Kluwer Academic, Dordrecht).

Freidovich, L., Mettin, U., Shiriaev, A. & Spong, M. [2009] "A passive 2-DOF walker: Hunting for gaits using virtual holonomic constraints," *IEEE Trans. Robot.* **25**, 1202–1208.

Fu, S. & Wang, Q. [2006] "Estimating the largest Lyapunov exponent in a multibody system with dry friction by using chaos synchronization," *Acta Mech. Sin.* **22**, 277–283.

Garcia, M., Chatterjee, A., Ruina, A. & Coleman, M. [1998] "The simplest walking model: Stability, complexity, and scaling," *J. Biomech. Eng.* **120**, 281–288.

Grizzle, J., Chevallereau, C., Sinnet, R. & Ames, A. [2014] "Models, feedback control and open problems of 3D bipedal robotic walking," *Automatica* **50**, 1955–1988.

Kunze, M. [2000] "On Lyapunov exponents for non-smooth dynamical systems with an application to a pendulum with dry friction," *J. Dyn. Diff. Eqs.* **12**, 31–116.

Kuo, A. [1999] "Stabilization of lateral motion in passive dynamic walking," *Int. J. Robot. Res.* **18**, 917–930.

Kuznetsov, Y. A., Rinaldi, S. & Gragnani, A. [2003] "One-parameter bifurcations in planar Filippov systems," *Int. J. Bifurcation and Chaos* **13**, 2157–2188.

La Herra, P., Shiriaev, A., Freidovich, L., Mettin, U. & Gusev, S. [2013] "Stable walking gaits for a three-link planar biped robot with one actuator," *IEEE Trans. Robot.* **29**, 589–601.

Leine, R. I., van Campen, D. H. & van de Vrande, B. L. [2000] "Bifurcations in nonlinear discontinuous systems," *Nonlin. Dyn.* **23**, 105–164.

Leine, R. I. & Nijmeijer, H. [2004] *Dynamics and Bifurcations of Non-Smooth Mechanical Systems* (Springer, Berlin, Heidelberg).

Leonov, G., Kuznetsov, N. & Vagaitsev, V. [2011] "Localization of hidden Chua's attractors," *Phys. Lett. A* **375**, 2230–2233.

Leonov, G. A. & Kuznetsov, N. V. [2013] "Hidden attractors in dynamical systems. From hidden oscillations in Hilbert–Kolmogorov, Aizerman, and Kalman problems to hidden chaotic attractor in Chua circuits," *Int. J. Bifurcation and Chaos* **23**, 1330002-1–69.

Li, S., Ma, W., Zhang, W. & Hao, Y. [2016a] "Melnikov method for a class of planar hybrid piecewise-smooth systems," *Int. J. Bifurcation and Chaos* **26**, 1650030-1–12.

Li, S., Shen, C., Zhang, W. & Hao, Y. [2016b] "The Melnikov method of heteroclinic orbits for a class of planar hybrid piecewise-smooth systems and application," *Nonlin. Dyn.* **85**, 1091–1104.

Licskó, G. & Csernák, G. [2014] "On the chaotic behaviour of a simple dry-friction oscillator," *Math. Comput. Simul.* **95**, 55–62.

Lynnyk, V. & Čelikovský, S. [2010] "On the anti-synchronization detection for the generalized Lorenz system and its application to secure encryption," *Kybernetika* **46**, 1–18.

Majumdar, A., Ahmadi, A. & Tedrake, R. [2013] "Control design along trajectories with sums of squares programming," *Proc. 2013 IEEE Int. Conf. Robotics and Automation* (*ICRA*) (Karlsruhe, Germany), pp. 4054–4061.

McGeer, T. [1990] "Passive dynamic walking," *Int. J. Robot. Res.* **2**, 62–82.

Pchelkin, S., Shiriaev, A., Freidovich, L., Mettin, U., Gusev, S., Kwon, W. & Paramonov, L. [2015] "A dynamic human motion: Coordination analysis," *Biol. Cybern.* **109**, 47–62.

Shi, L., Zou, Y. & Küpper, T. [2013] "Melnikov method and detection of chaos for non-smooth systems," *Acta Math. Appl. Sin., Engl. Ser.* **29**, 881–896.

Shiriaev, A., Perram, J. & Canudas-de Wit, C. [2005] "Constructive tool for orbital stabilization of underactuated nonlinear systems: Virtual constraints approach," *IEEE Trans. Autom. Contr.* **50**, 1164–1176.

Shiriaev, A., Robertsson, A., Perram, J. & Sandberg, A. [2006] "Periodic motion planning for virtually constrained Euler–Lagrange systems," *Syst. Contr. Lett.* **55**, 900–907.

Shiriaev, A., Freidovich, L. & Spong, M. [2014] "Controlled invariants and trajectory planning for underactuated mechanical systems," *IEEE Trans. Autom. Contr.* **59**, 2555–2561.

Song, G. & Zefran, M. [2006a] "Stabilization of hybrid periodic orbits with application to bipedal walking," *Proc. 2006 American Control Conf.* (Minneapolis, Minnesota), pp. 2504–2509.

Song, G. & Zefran, M. [2006b] "Underactuated dynamic three-dimensional bipedal walking," *Proc. 2006 IEEE Int. Conf. Robotics and Automation* (*ICRA*) (Orlando, Florida), pp. 854–859.

Spong, M. & Bullo, F. [2005] "Controlled symmetries and passive walking," *IEEE Trans. Autom. Contr.* **50**, 1025–1031.

Stefański, A. [2000] "Estimation of the largest Lyapunov exponent in systems with impacts," *Chaos Solit. Fract.* **11**, 2443–2451.

Stefański, A. & Kapitaniak, T. [2000] "Using chaos synchronization to estimate the largest Lyapunov exponent of nonsmooth systems," *Discr. Dyn. Nat. Soc.* **4**, 207–215.

Stefański, A. & Kapitaniak, T. [2003] "Estimation of the dominant Lyapunov exponent of non-smooth systems on the basis of maps synchronization," *Chaos Solit. Fract.* **15**, 233–244.

Westervelt, E., Grizzle, J., Chevallereau, C., Choi, J. & Morris, B. [2007] *Feedback Control of Dynamic Bipedal Robot Locomotion* (CRC Press, Berlin).